

THESIS ON NATURAL AND EXACT SCIENCES B60

**Electrochemical Deposition of CuInSe₂ Thin Films
for Photovoltaic Applications**

JULIA KOIS

TALLINN UNIVERSITY OF TECHNOLOGY

Faculty of Chemical and Material Technology

Department of Materials Science

Chair of Semiconductor Materials Technology

Dissertation for the Degree of Doctor of Philosophy in Natural Sciences will be examined at Tallinn University of Technology

Supervisor: Prof. Enn Mellikov

Opponents: Prof. Dieter Meissner, University of Applied Sciences, Wels, Austria
DSc. Mati Arulepp, Tartu Tehnoloogiad OÜ, Riia mnt. 71-1, 51014, Tartu

Defence: 14th of December, 2006, at 13.00
Lecture hall: V-103
Tallinn University of Technology, Ehitajate tee 5, 19086, Tallinn

Declaration:

I declare that this doctoral thesis is my original research work. It is being submitted for the Degree of Doctor of Philosophy in Natural Sciences in Tallinn University of Technology. The thesis has not been submitted before for any degree or examination in other universities.

Julia Kois

Copyright: Julia Kois, 2006

ISSN 1406-4723

ISBN 9985-59-672-2

LOODUS- JA TÄPPISTEADUSED

**CuInSe₂ õhukesed kiled elektrokeemilise
sadestamise meetodil**

JULIA KOIS

LIST OF PUBLICATIONS

This work is based on the following original publications, which are referred to in the text by their Roman numerals. In addition, the kinetics of deposition and annealing are discussed on the basis of partly published results.

- I. J. Kois, S. Bereznev, E. Mellikov and A. Öpik, Electrodeposition of CuInSe₂ thin films onto Mo-glass substrates, *Thin Solid Films*, Vol. 511-512, 26 July 2006, pp 420-424.
- II. J. Kois, S. Bereznev, O. Volobujeva, E. Mellikov, Electrochemical Etching of Copper Indium Diselenide Surface, The E-MRS 2006 Spring Meeting Nice (France), from May 29 to June 2, 2006, *Thin Solid Films*, accepted.
- III. Julia Kois, Sergei Bereznev, Enn Mellikov, and Andres Öpik, Photovoltaic structures formed by thermal annealing of electrodeposited CuInSe₂ in H₂S, *Proceedings of the Estonian Academy of Sciences, Chemistry*, Vol. 52 No. 2 June 2003, pp. 51–58.
- IV. J. Kois, S. Bereznev, J. Raudoja, E. Mellikov and A. Öpik, Glass/ITO/In(O,S)/CuIn(S,Se)₂ solar cell with conductive polymer window layer, *Solar Energy Materials and Solar Cells*, Vol. 87, Issues 1-4, May 2005, pp. 657-665.
- V. S. Bereznev, J. Kois, I. Golovtsov, A. Öpik and E. Mellikov, Electrodeposited (Cu–In–Se)/polypyrrole PV structures, *Thin Solid Films*, Vol. 511-512, 26 July 2006, pp. 425-429.
- VI. S. Bereznev, J. Kois, E. Mellikov, A. Öpik and D. Meissner, CuInSe₂/Polypyrrole Photovoltaic Structure Prepared by Electrodeposition, *Proceedings of 17th European Photovoltaic Solar Energy Conference (Munich, Germany, October 22-26, 2001)*, 1 (2002), pp. 160-163.
- VII. S. Bereznev, J. Kois, E. Mellikov, A. Öpik, CuInSe₂/Polyaniline Photovoltaic Structure, *Proceedings of Baltic Polymer Symposium 2001, Tallinn, Estonia, October 11-12, 2001*, pp. 148-154.

AUTHOR'S OWN CONTRIBUTION

The contribution by the author to the paper included in thesis is a followings:

- I. Electrodeposition of thin films and XRD measurements, analysis, major part of writing.
- II. Electrodeposition of thin films, thermal treatment and etching of thin films, voltammetry analysis, major part of writing
- III. Electrodeposition of thin films, thermal treatment of thin films, XRD, electrical and optical analysis, major part of writing
- IV. Electrodeposition of thin films, thermal treatment of CuInSe₂ thin films, electrical and optical analysis, part of writing
- V. Electrodeposition of thin films, thermal treatment of CuInSe₂ thin films, XRD analysis, part of writing
- VI. Electrodeposition of thin films, thermal treatment of CuInSe₂ thin films, minor part of writing
- VII. Electrodeposition of thin films, thermal treatment of CuInSe₂ thin films, minor part of writing

Deposition of polymer thin films and metallic contacts, SEM, EDX, XRD analysis, electrical and optical measurement were done by co-workers.

LIST OF USED SYMBOLS AND ABBREVIATION

$[X]^{el}$	concentration at the electrode surface
$[X]$	concentration in the bulk of solution
a	activity
ALD	Atomic Layers Deposition
CBD	Chemical Bath Deposition
D	diffusion coefficient
E	electrode potential
E_0	$E_0 = E^0 + (RT/nF) \ln(a_{M^{n+}} / a_M)$
E^0	standard potential
EBS	Electron BackScattered In-lens detector (used for compositional contrast)
EDX	Energy Dispersive X-ray analysis
E_g	band gap
F	Faraday constant
FF	fill factor
I_{sc}	circuit current density
ITO	Indium tin oxide doped SnO ₂ :In
J	total density of flux of reacting species
j_c	density of cathodic currents
j_d	diffusion current
j^{lim}	limited migration current density
j_m	migration current density
k	rate constant
n	number of electrons required for the reaction
NHE	Normal Hydrogen Electrode
PANI	polyaniline
PEDOT	poly(3,4-ethylenedioxythiophene)
PPy	polypyrrole
PSS	polystyrenesulfonate
R	gas constant
SCE	Saturated Calomel Electrode
SE	Secondary Electrons In-lens detector of SEM (used mostly to resolve topographic info)
SEM	Scanning Electron Microscope
SME	Sulfate Mercurous Electrode
T	absolute temperature
u	mobility of species
UV-Vis	Ultraviolet-visible spectroscopy
V_{oc}	open circuit voltage
z	charge of ion
α	absorption coefficient
α	ratio between selenium and copper fluxes
β	asymmetry parameter, evaluating the asymmetry the free energy potential curve with respect to reactant and product.
δ	diffusion layer thickness
ΔG	free energy
E	electric field strength

CONTENTS

LIST OF PUBLICATIONS	4
LIST OF USED SYMBOLS AND ABBREVIATION	6
KOKKUVÕTE	9
ABSTRACT	10
1. INTRODUCTION	11
1.1. FUNDAMENTAL CONSIDERATIONS	12
1.1.1. THERMODYNAMICS OF ELECTROCHEMICAL DEPOSITION	12
1.1.2. KINETICS OF ELECTROCHEMICAL DEPOSITION	13
1.2. ELECTRODEPOSITION OF I-III-VI CHALCOPYRITES	15
1.2.1. CHEMISTRY OF ELECTRODEPOSITION OF CuInSe ₂	16
1.2.2. ELECTROLYTE COMPOSITION	18
1.2.3. POST- TREATMENTS OF ELECTRODEPOSITIED OF CuInSe ₂ FILMS	19
1.3. CHALCOPYRITE THIN FILM SOLAR CELLS	20
2. GOALS OF THE RESEARCH	21
3. EXPERIMENTAL	22
3.1. VOLTAMMETRIC STUDY AND ELECTRODEPOSITION OF FILMS	22
3.2. POST-DEPOSITION TREATMENTS OF FILMS	22
3.3. characterization of film	23
3.4. PREPARATION OF SOLAR CELLS	23
4. RESULTS	25
4.1. ELECTROCHEMICAL DEPOSITION OF CuInSe ₂ FILMS	25
4.1.1. CHEMICAL PROCESSES IN AN ELECTROCHEMICAL BATH	25
4.1.2. Film growth	25
4.1.2.1. THERMODYNAMIC ASPECT OF ELECTRODEPOSITION CuInSe ₂ FILMS	25
4.1.2.2.KINETIC ASPECT OF ELECTRODEPOSITION CuInSe ₂ FILMS	27
4.1.3. MORPHOLOGY OF DEPOSITED FILMS	33
4.2. POST-DEPOSITION TREATMENT	34
4.2.1. ANNEALING UNDER SE VAPOUR PRESSURE	34
4.2.2. THERMAL ANNEALING IN THE ATMOSPHERE OF H ₂ S	37
4.2.3. CHEMICAL AND ELECTROCHEMICAL ETCHINGS	37

4.3. CHARACTERIZATION OF THIN FILMS	39
4.4. SOLAR CELL STRUCTURES ON ELECTRODEPOSITED CuInSe ₂ FILMS	41
4.4.1. ITO/In(O,S)/ CuIn(S,Sex) ₂ PHOTOVOLTAIC STRUCTURE	41
4.4.2. ITO/In(O,S)/CuIn(S,Se) ₂ /polymers PHOTOVOLTAIC STRUCTURE	43
4.4.3. ITO/CuInSe ₂ /polymers PHOTOVOLTAIC STRUCTURES	44
CONCLUSIONS	46
ACKNOWLEDGEMENTS	47
REFERENCES	48
APPENDIX	53
CURRICULUM VITAE	116
ELULOOKIRJELDUS	118

KOKKUVÕTE

Päikeseenergeetika suuremastaabiline kasutamine elektrienergia tootmiseks nõuab suuri mahte ka päikesepaneelide tootmisel. Lahenduse selleks võivad anda õhukesekilelised tehnoloogiad, mis võimaldavad luua suurtes kogustes selleks vajalikke odavaid ja kergeid päikesepaneele kasutades alusmaterjalidena kas klaasi, püüamiidset kilet ja õhukesi roostevabast terasest lehti. Elektrokeemiline sadestamine omab väga head potentsiaali odavate õhukesekileliste tööstuslikuks tootmiseks tänu elektrokeemilise protsessi kergele kontrollivõimalusele ja aparatuursele lihtsusele

Dissertatsioon annab ülevaate õhukesekileliste päikeseelementide elektrokeemilise sadestamise tänapäeva tasemest maailmas kontsentreerudes enda eksperimentaalses osas üheetapilise elektrokeemilise sadestamise tehnoloogia ning saadud materjalide omadusi optimiseerivate järgnevate termitsetööstustega seotud sõlmprobleemidele.

Dissertatsioonis antakse ülevaate CuInSe_2 õhukeste kilede termodünaamikast ning elektrokeemiline sadestusprotsessi mehhanismist ja kineetikast. On näidatud, et CuInSe_2 õhukeste kilede sadestamise mehhanism on kujutatav läbi rea järgnevate üksteistest sõltuvate reaktsioonide. CuInSe_2 moodustumise esimeseks etapiks on erinevate $\text{Cu} + \text{Se}$ ühendite moodustumine, millele järgnevad reaktsioonid indiumi osavõtul ja CuInSe_2 moodustumine. $\text{Cu} + \text{Se}$ ühendite moodustumise kineetika on kontrollitud Se ja Cu osakeste difusioonikineetikaga, indiumi osavõtul toimuvate reaktsioonide kulg on määratud kasutatava elektrokeemilise sadestamise potentsiaaliga. Dissertatsioonis on toodud mudel, mis seob Cu , In ja Se voogude suurused ja nende elementide suhtelised kontsentratsioonid saadavates kiledes. Läbiviidud arvutused võimaldasid esitada töös erinevate elementide kontsentratsioonid lõpp-produktis vastavate jaotusdiagrammina. Elektrokeemilisel sadestamisel saadud kilede morfoloogia on määratud nende koostiskristallide nukleatsioonikiirusega, mis omakorda sõltub sadestamisel kasutatud ülepingselt ja lahuses olevate kile komponentide massitranspordi kiirusest.

Üheastmelises elektrokeemilises protsessis saadud kiled vajavad täiendavaid termitsetööstusi optiliste ja elektriliste omaduste optimiseerimiseks. Dissertatsioonis on näidatud, et lisaks muutustele optilistes omadustes muutub termitsetööstustes tugevalt kilede morfoloogia ja kristallstruktuur. On tõestatud, et CuInSe_2 elektrokeemiliselt sadestatud kilede küsitlemisel Se sisaldavas keskkonnas saadavate kilede morfoloogia ja kristallstruktuur on määratud lähtekile koostise ja kasutatava Se aururõhuga. On näidatud, et kõrgetel Se aururõhkudel saadakse Se -rikkad faasid, mis temperatuuridel ca 500 C on sulas olekus ja soodustavad reaktsioonist osavõtivate osakeste difusiooni. Termiline käsitlus H_2S voolus 30 minuti jooksul viib uue ühendi $\text{CuIn}(\text{S},\text{Se})_2$ tekkele. Töös on välja töötatud meetodid termitsetööstuste käigus kile pinnale moodustunud Cu_2Se faaside eemaldamiseks nende söövitamisel KCN vesilahuses ja elektrokeemilisel söövitamisel nii happelistes kui ka aluselistes lahustes.

Elektrokeemilised CuInSe_2 kiled omavad otsest tsooniskeemi ja keelutsooni, mida on võimalik kontrollida kilede keemilise koostisega ja mis varieerub vahemikus 0.8-1.1 eV. Termilised käsitlused H_2S voos viivad keelutsooni suurenemiseni kuni väärtusteni 1.5eV.

Dissertatsiooni tegemisel saadud elektrokeemiliselt sadestatud kilede baasil on loodud kahte erinevat tüüpi PV struktuure, vastavalt $n\text{-In}(\text{O},\text{S})/p\text{-CuIn}(\text{S},\text{Se})_2$ ülemineku struktuurid ja hübriidsed struktuurid $n\text{-CuInSe}_2$ pooljuht / orgaaniline pooljuht p -tüüpi juhtiv polümeer. Saadud $n\text{-In}(\text{O},\text{S})/p\text{-CuIn}(\text{S},\text{Se})_2$ struktuurid omavad tühijooksupinget (V_{oc}) = 373 mV, lühisvoolu (I_{sc}) = 1 mA/cm^2 and täitumiskoeffitsienti (FF) ~25%. Parimad struktuurid n -tüüpi CuInSe_2 õhukeste kilede ja p -tüüpi orgaaniliste polümeeride (polüürooli) baasil omavad V_{oc} = 92 mV ja I_{sc} = 1.70 mA/cm^2 .

ABSTRACT

Large scale PV (Photovoltaic) energy production needs large-area solar-cell installations. Thin-film solar cell deposition (besides wafer-based Si technology) on soda-lime glass, stainless steel, or polyamide substrates is a cheap technology, which would make these solar cells truly lightweight and large area. The benefits electrodeposition can provide are convenient and inexpensive production of large-area solar cells, utilizing a technology readily adaptable to industrial production.

This thesis reviews the state of the art of electrochemical deposition of chalcopyrite absorber layers for thin film solar cells and summarizes our results of investigation in the field of one-step electrodeposition and different post-treatments of CuInSe₂ electrodeposited thin films.

This thesis presents a new approach to the thermodynamics and kinetics constituent of the electrodeposition mechanism of CuInSe₂. It will be shown that the mechanism CuInSe₂ phase formation goes through a number of consecutive reactions. The formation of Cu + Se phases precedes the assimilation of indium and CuInSe₂ compound formation. Under the conditions of electrodeposition all three elements in the one-step electrochemical deposition process, the formation of Cu+Se phases are controlled by the diffusion of selenium and copper species, the insertion of indium into the film depends on the applied potential.

The thesis describes associated model used to determine the fluxes of copper, indium and selenium species to the cathode and relative concentrations of deposited solid phases. The results of computations enable us to build the distribution diagram of the final products.

It is shown that the morphology of electrodeposited films is determined by the nucleation rate of crystals (is the function of overpotential) and the rate of mass transport of solute species.

In order to achieve the desired semi-conducting properties, the precursor films need to be thermally annealed. Change of annealing conditions (temperature, time and atmosphere of annealing) allows us to control the morphology and optical and electrical properties of annealed films and to prepare films and later solar cell structures with tailored technical parameters. The structure and morphology of CuInSe₂ thin films depends on the precursor film composition and the pressure of Se vapour. High Se pressure leads to the formation of Se-rich binary compounds, which at 500 °C are believed to be in a quasi-liquid state and provide high diffusion of reactive compounds. The annealing in H₂S flow gas at temperature 450°C during 30 min leads to the formation of CuIn(S,Se)₂ compound. The chemical etching in KCN and electrochemical etching in acidic and alkaline medium was used for removing Cu₂Se phases from the surface of the prepared and annealed films.

As-deposited CuInSe₂ thin films showed direct transition with bandgap energy in the range of 0.8-1.1 eV depending on precursor composition. The as-deposited Cu-rich film with summary virtual composition 24 at% Cu, 24 at% In and 52 at% Se have $E_g = 0.87$ eV, the film with summary composition 11 at% Cu, 37 at% In and 52 at% Se has $E_g = 1.0$ eV. Optical properties of electrodeposited CuInSe₂ films annealed in the atmosphere of H₂S indicate to an increase of bandgap up to 1.5eV.

This thesis presents two types of solar cells prepared by help of electrochemical deposition of precursor CuInSe₂ thin films: photovoltaic structure on the base of *n*-In(O,S)/*p*-CuIn(S,Se)₂ junction and combined inorganic *n*-CuInSe₂/*p*-polymer photovoltaic structure. For cells based on CuInSe₂ films treated with H₂S, the highest open circuit voltage (V_{oc}) was 373 mV, whereas the density of short circuit current (I_{sc}) was 1mA/cm² and the fill factor (FF) was 25%. The best structure based on *n*-type of CuInSe₂ thin films and *p*-type conductive polymer (polypyrrole) shows the values of $V_{oc} = 92$ mV and $I_{sc} = 1.70$ mA/cm² under white light illumination with 50 mW/cm²

1. INTRODUCTION

To be a successful player on the electricity market, the price of a kWh of energy produced by PV panels will have to fall and of PV panel production will have to expand significantly. One of the most promising strategies for lowering of the cost of PV energy is the use of thin-film technologies in which thin films of photo-active materials (typically less than 5 μm in thickness) are deposited onto inexpensive large-area substrates. Thin film solar cell materials require less material to generate a given amount of power that makes alternatives more attractive as compared to single crystalline devices. Three perspective thin film solar cell materials: copper indium diselenide (CuInSe_2), copper indium disulfide (CuInS_2) and copper gallium diselenide (CuGaSe_2) have high absorption, near optimum for the solar spectrum in space (AM0) and on the surface of Earth (AM1.5). NREL (National Renewable Energy Laboratory (USA))^a scientists have achieved efficiencies up to 19.2 % with CuInSe_2 absorber in the laboratory cell. The best efficiency of a thin-film solar cell up to December 2005 was 19.5 % by help of Cu(In,Ga)Se_2 absorber. Higher efficiencies (around 30%) could be obtained by using optics to concentrate the incident light. The best conversion efficiency for Cu(In,Ga)Se_2 cells on flexible polyamide substrates, obtained by Tiwari et al. at the ETH^b, Switzerland, in 2006, has the value of 14.1%. However, current thin film cell technologies are limited by either: (1) the ultimate efficiency that can be achieved with the material device and structure or (2) the requirement for high-temperature deposition processes.

Electrodeposition of semiconducting materials thus represents a new challenge, since this method presents interesting characteristics for a large area, low cost and generally low temperature and soft processing of materials. An advantage of this electrically driven process is a chance of precise control of the growth process. Other attractive advantages include: (1) purification materials occurs during electrodeposition because of differences in the depositing potential of components, (2) a wide range of compounds and elements can be electrodeposited and (3) electrolysis is convenient for epitaxial deposition since growth occurs uniformly over the same area. Electrodeposition has already been shown to be a promising approach to produce efficient, low-cost CuInSe_2 and Cu(In,Ga)Se_2 solar cells. Efficiencies in the range of 6–7% have been reported for the so-called one-step electrodeposition route [1].

This doctoral thesis reviews the state of art in CuInSe_2 absorber layer preparation in thin film solar cells by electrodeposition. Author's approaches to the basic aspects of CuInSe_2 thin film electrodeposition and post-treatment of the obtained films together with obtained experimental results are also presented.

^a <http://www.nrel.gov/>

^b <http://www.solid.phys.ethz.ch/>

1.1. FUNDAMENTAL CONSIDERATIONS

1.1.1. THERMODYNAMICS OF ELECTROCHEMICAL DEPOSITION

Electrodeposition of elemental semiconductors. Electrodeposition of metals involves the reduction of metal ions from electrolytes. In general terms, the reaction in the aqueous medium involved in electrodeposition is:



The change in free energy ΔG is given by [2]

$$\Delta G = -\Delta G^0 + RT \ln(a_{M^{n+}}/a_M), \quad \text{Eq.2}$$

where R is the gas constant, T is the absolute temperature, $a_{M^{n+}}$ and a_M are the activities of M^{n+} in the electrolyte and of M in the deposit, respectively. E^0 is the standard potential and is defined [3] by:

$$E^0 = -\Delta G^0/nF, \quad \text{Eq.3}$$

where F is the Faraday constant and n is the number of electrons required for the reduction. Thus, the potential where the reduction reaction (Eq.1) occurs can be estimated from the Nernst equation:

$$E_0 = E^0 + (RT/nF) \ln(a_{M^{n+}}/a_M), \quad \text{Eq.4}$$

where E^0 is the standard potential for the reduction to form M^c .

Electrodeposition of M can occur at potentials more negative than the equilibrium potential. The deviation from equilibrium is defined as the overpotential η .

$$\eta = E - E^0 \quad \text{Eq.5}$$

Electrodeposition of alloys and compound semiconductors. The situation is more complicated in the case of compound semiconductor formation such as CdTe. In the conditions of alloy or compound formation, the reversible potential of a less noble metal alloyed should be more positive than that of a pure metal. The shift of the potential is a constant value for the formation of a compound, but it varies depending on the composition for alloy formation. Thus, the deposition potential of Cd is shifted by an amount $-\Delta G/2F$, which provides the free energy of reaction to produce CdTe [4,5].

^c For simplicity, the interactions of solute ion M^{n+} with the solvent or with complex-forming ligands have been ignored.

1.1.2. KINETICS OF ELECTROCHEMICAL DEPOSITION

Briefly some important factors that influence the deposition of semiconductors are described below.

Rate of the electron transfer reaction, i.e. the oxidation-reduction kinetic, could be indicated by the exchange current density. The reaction rate of cathodic reduction could be represented by

$$j_c = -n F k [X]^{el} \quad \text{Eq.6}$$

$[X]^{el}$ is the concentration of M^{n+} at the electrode surface, k is the rate constant, j_c is the density of partial cathodic currents. The electrochemical rate constant k^* of the reaction is determined by

$$k^* = k \exp\left\{- (1-\beta) \frac{nF}{RT} (E-E^0)\right\} \quad \text{Eq.7}$$

E is the cathodic potential, E^0 is the standard redox potential of the reaction, β is the asymmetry parameter, evaluating the asymmetry of the free energy potential curve with respect to the reactant and product.

Mass transport of the species can be calculated from the corresponding current density j , thus

$$J = j/n F, \quad \text{Eq.8}$$

where J is the total density of flux of the reacting species. The total current density j is determined by the balance equation.

$$j = j_m + j_d + j_{kv}, \quad \text{Eq.9}$$

where j_m is migration, j_d is diffusion and j_{kv} is the convection component of current density j . The migration current density j_m is

$$j_m = -z c u E \quad \text{Eq.10}$$

E is the electric field strength, $[X]$ is the concentration of M^{n+} in the bulk of solution, u is the mobility of species and z is the charge of the ion. The diffusion current j_d has the value

$$j_d = -nF \frac{D}{\delta} ([X] - [X]^{el}), \quad \text{Eq.11}$$

where D is the diffusion coefficient, δ is diffusion layer thickness. According to the equation of Nernst –Planck

$$j = j_m + j_d = -z c u E - nF \frac{D}{\delta} ([X] - [X]^{el}) \quad \text{Eq.12}$$

In most cases the migration component is too small, since solutions used in the electrochemical system are too conductive and diffusion dominates.

If the electrode surface is totally depleted by species M^{n+} , then $[X] \gg [X]^{el}$. The maximal current, corresponding to the limiting current could be given as

$$j^{lim} = - nF \frac{D}{\delta} [X] \quad \text{Eq.13}$$

The thickness of the diffusion layer in this case is proportional to $D^{1/3}$.

The nucleation rate of crystals is a function of the overpotential and it also influences the nature of the electrodeposition process and the final product.

1.2. ELECTRODEPOSITION OF I-III-VI CHALCOPYRITES

The electrodeposition of I-III-VI elements based semiconductors started in the 1980s and has been advancing up to today. Interest in electrodeposition is demonstrated by growth in publication in the domain. The Figure 1 shows the dynamics of number of publications in the electrodeposition of CuInSe_2 and Cu(In,Ga)Se_2 (source: INSPEC and Current Contents).

The deposition of stacked elemental layers (Cu, In, Ga, Se) with subsequent thermal treatment is the simplest way for CuInSe_2 or Cu(In,Ga)Se_2 thin film preparation. The thickness of each layer is easily controlled by coulometry, the overall composition of the precursor films thus is also controlled [6,7]. The plating of indium layer on Cu-type [8] or deposition copper/indium bilayers [9,10,11,12], which are then reacted thermally with a selenium (or sulfur) atmosphere, is widely used for CuInSe_2 , CuInS_2 [13] and Cu(In,Ga)Se_2 preparation [14].

Papers devoted to electrodeposition of indium selenide [15,16] and copper selenide [17,18] revealed the possibility of CuInSe_2 film production from pseudobinary chalcogenide layers [19,20,21,22].

Bhattacharya [23] was the first to electrodeposit CuInSe_2 thin films from a unique electrolyte containing all three constitution elements. This process, named codeposition or one-step deposition, is the most widely investigated process today [24,25,26].

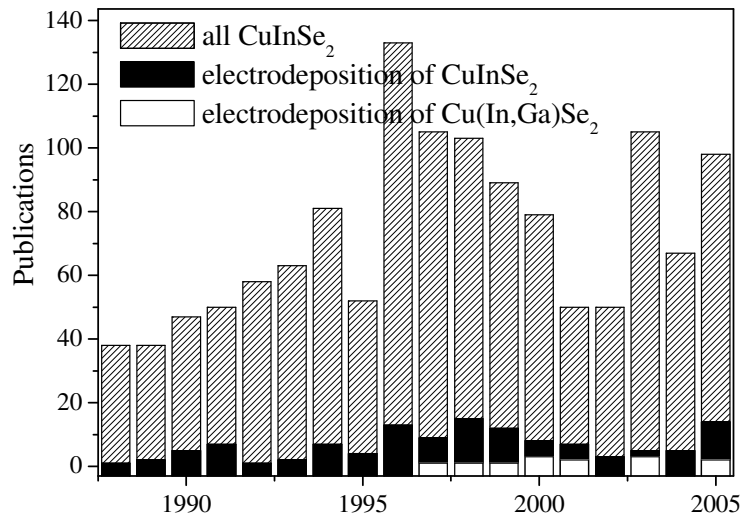


Figure 1. Number of published papers from Current Contents data base (1985–September 2006)

Successful attempts to produce one-step electrodeposition of Cu(In,Ga)Se_2 [27,28,29,30,31,32] and CuIn(S,Se)_2 [33] have been made during the last years. Additionally several papers covering the electrodeposition of other thin film based chalcopyrites I-III-VI, such as CuInTe_2 [34] and CuIn(Se,Te)_2 [35], have been published.

1.2.1. CHEMISTRY OF ELECTRODEPOSITION OF CuInSe₂

As three different components are involved, the electrodeposition of CuInSe₂ is a special case of the codeposition of compound semiconductors. The reaction mechanisms of the formation CuInSe₂ electrodeposited films have been studied in several articles [36,37,38].

The combined diagram of corrosion, immunity and passivation domains of copper, indium and selenium was used by Sing (1985) [39] to define the conditions of codeposition of the elements. The reduction potentials of elements range from +0.75V vs. NHE (Normal Hydrogen Electrode) and selenium 0.34V for Cu up to -0.34V for In.

Figure 2 shows the simplest model of CuInSe₂ formation used in a number of articles [40,41]. The kinetic model for this process has been developed by S. M. Babu (1991) [42].

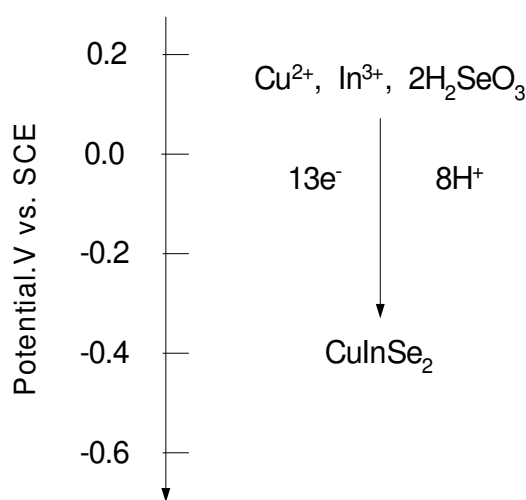


Figure 2. Electrochemical diagram showing the model of CuInSe₂ formation. The solution is supposed to be acidic under standard conditions. The potential is given with respect to the Saturated Calomel Electrode (SCE, -0.24V vs. NHE).

It was found that in the process of CuInSe₂ codeposition, the deposition potential of copper and indium is shifted to a more positive value. Thin films of CuInSe₂ prepared by the electrochemical deposition technique are generally a mixture of several phases (copper selenide and indium selenide) in a nanocrystalline and/or amorphous state [43,44,45].

The thermodynamic treatment of underpotential formation of compound semiconductors has been reported by Kroger [4]. Reactions accompanying the electrodeposition of binary copper selenium compounds were studied by Massaccesi [17] and Lippkow [18]. In her work Massaccesi [17] determined the dependence of deposit composition on the ratio of selenium and copper fluxes (r_J , later marked as α).

The models proposed by Ueno (1988) [46] and Molin (1993) [47,48] explain the underpotential incorporation of indium through different reactions (Figure 3 and Figure 4).

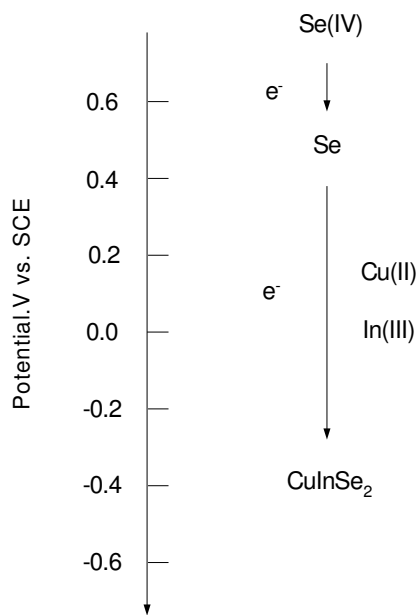


Figure 3. Electrochemical diagram showing the model of CuInSe_2 formation. Under standard conditions, the solution is supposed to be acidic, by Ueno [46]

OR

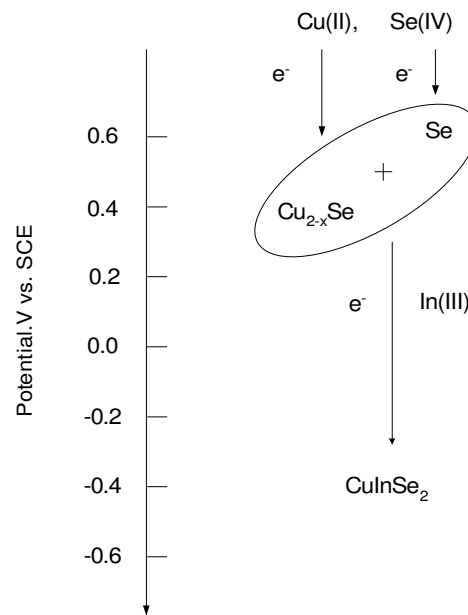


Figure 4. Electrochemical diagram showing the model of CuInSe_2 formation. Under standard conditions, the solution is supposed to be acidic, by Molin [48]

Mishra and Rajeshwar (1988) [37] proposed a mechanism in which CuInSe_2 is formed by the reduction of non-stoichiometric cuprous selenide Cu_{2-x}Se into copper and H_2Se , which reacts with the In(III) in the solution and with non-reduced Cu_2Se to form CuInSe_2 . They were the first to map the stability regimes of system $\text{Cu-Se-H}_2\text{O}$ using Pourbaix analyses [37].

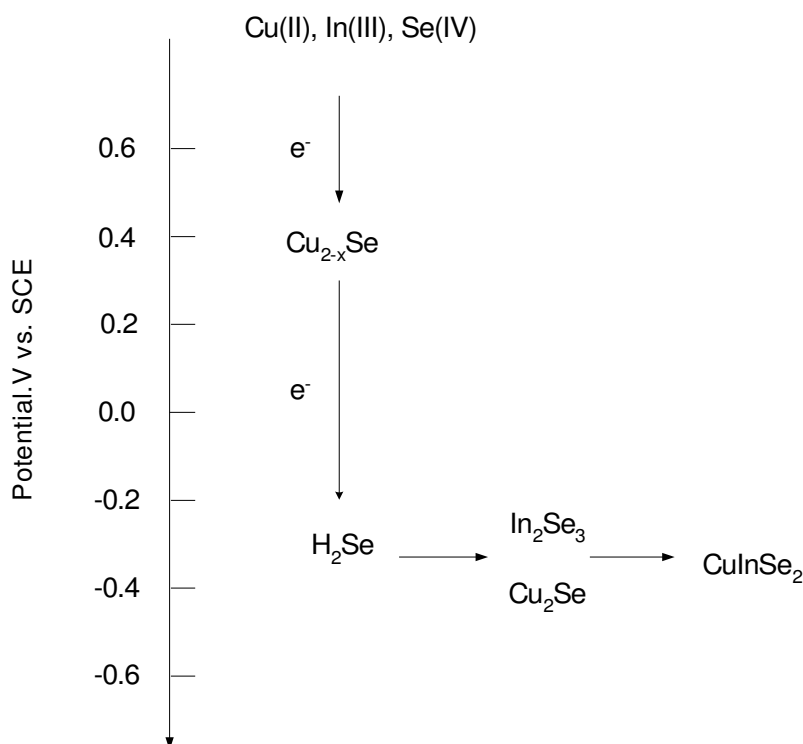


Figure 5. Electrochemical diagram showing the model of CuInSe_2 formation. Under standard conditions the solution is supposed to be acidic, by Mishra [37]

The possibility to control the composition and the deposition mechanism by the flux ratio (α) to the electrode was suggested first by Thouin and Massaccesi (1993) [17,36,45]. The dependence of phase composition on the deposition potential and various values of the flux ratio α are shown in Figure 6 [16,43]. The kinetic model of CuInSe_2 deposition that is under diffusion control for Cu and Se species was developed in articles [38,43 and 37].

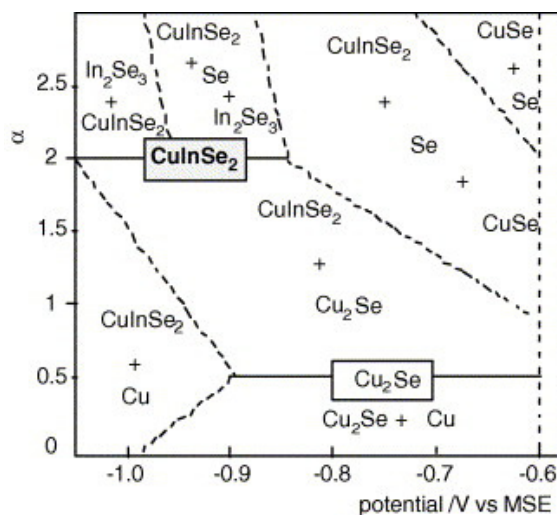


Figure 6. Electrochemical phase diagram showing the composition of one-step electrodeposited films in the Cu–In–Se system from acidic solutions as a function of the electrodeposition potential and the flux ratio between selenium(IV) and copper(II) ionic species in solution [49 ,50]. The potentials are referred to the Sulfate Mercurous Electrode (MSE, -0.65 V vs NHE).

1.2.2. ELECTROLYTE COMPOSITION

With the reference to the literature, one-step electrodeposition of CuInSe_2 usually carried out from an aqueous acidic solution containing simple compounds of Cu(II) and In(III), most often sulfates [36,46,37] and chlorides [51,19,52,6]. The most popular Se precursor is SeO_2 (in mildly acidic solutions it is in the form of H_2SeO_3), but Na-selenosulfate [53] has been used as Se containing precursor too. As supporting electrolytes sulfates (K_2SO_4) [54,36] or chlorides (LiCl [55]) could be used. To prevent the precipitation of indium hydroxides, the acidity of solution has to be held at $\text{pH} < 2$.

The reduction potential of some ions could noticeably vary, depending on the solvents used or complexing agents added to the electrolyte [3]. In order to bring the potentials of the three elements Cu, In and Se closer, electrodeposition in non-aqueous media, such as triethanolamine [56,23] and glycine [57], has been studied by several groups. Citrate, triethanolamine ions or complexing ethylenediaminetetraacetic acid (EDTA) are some prospective additives reported for the electrochemical deposition of CuInSe_2 [47,58,45]. These species act as complexing agents for metallic ions or as surface modifiers, which affect the structure of the films and/or electrochemical kinetics.

Stratieva [59] and Kemell [60] used Cu(I) ions containing aqueous solutions that allow for a marked shift in the deposition potential of elemental copper as close as possible to that of

indium. Due to the limited solubility of Cu(I) compounds and the instability of the free Cu(I) ions in aqueous solutions, copper ions were complexed with thiocyanate that is a strong complexing agent of copper(I).

1.2.3. POST- TREATMENTS OF ELECTRODEPOSITIED OF CuInSe₂ FILMS

As indicated in the Section 1.2.1, as-electrodeposited precursor films lack the quality needed for PV cell use. The films are polycrystalline by nature and as a rule contain a mixture of several phases. Thermal treatment is ordinarily used to improve crystallinity, to lower electrical conductivity and to increase grain size.

The physical properties of bulk CuInSe₂ are strongly dependent on compositional deviations from the ideal stoichiometry and the precipitation of secondary phases [61,62]. Either *p*- or *n*- type CuInSe₂ crystals could be grown from the melt via stoichiometry control through introduction of native defects, without introducing extrinsic impurities [63]. This has been observed in single crystals as well as in thin films [64].

Annealing. The parameters of the thermal treatment process depend on the nature of precursor films. Direct electrodeposition provides Cu, In and Se constituents from the same electrolyte (one step process), but the obtained films are polycrystalline by nature and have a mixture of several phases. Annealing is required to complete reactions between the constituents and recrystallization of the formed CuInSe₂ films.

The level of crystallization in the atmosphere of gaseous Se strongly depends on selenium vapour pressure (usually controlled by the temperature of Se source) [65]. CuInSe₂ crystals grown under the applied Se vapour pressure higher than 5 Torr have Se-rich compositions, while the crystals grown under the applied Se vapour pressure less than 5 Torr have (CuIn)-rich compositions [66].

Electrodeposited precursor film in selenium vapour was annealed in close chamber [67] and [70] at temperature 500°C during the period from few minutes up to one hour [68] with the aim to complete formation of CuInSe₂ and in homogenization of composition of the films [69]. Annealed electrodeposited films demonstrated the improvement of electronic quality of material [,24,67] and remarkable improvement a crystallinity [70,71,72,24,67].

Annealing of CuInSe₂ and Cu(In,Ga)Se₂ precursors under neutral atmosphere (Ar, N₂) or vacuum leads to the recrystallization of films and as a result improves of the structural and optical properties. The effect is more pronounced if annealing temperature is increased up to 350°C [73,74,75] and [49,76,77,78,79]. However short time (around 20 min) vacuum annealing results in insufficient crystallinity of the film, and in unsatisfactory electronic properties [80,81,82,83].

Sulfurization is one of the methods to modify film surface for the improvement the properties of solar cell devices based on CuInSe₂ [84,85]. Rapid thermal processing in H₂S atmosphere with processing temperatures ranging from 350 to 550°C was used to sulfurize Cu(In,Ga)Se₂ surface of absorber layers [85].

Etching. CuInSe₂ films prepared with an excess of Cu need an additional processing step to remove separate binary phases like Cu₂Se from the surface. The prevalent method for removing segregated Cu-Se and Cu-S phases is chemical etching in KCN solutions [86,87]. Another approach to modify the surface is an exposure of the surface to strong oxidants, such as Br [86], H₂O₂ [88], permanganates [88] or complexes [89]. Removal of segregated phase by electrochemical oxidation has been investigated by several research groups additionally [90,91,92].

1.3. CHALCOPYRITE THIN FILM SOLAR CELLS

A typical thin film solar cell is shown in Figure 7. Cu(In,Ga)Se₂ module fabrication has the same advantageous features of thin-film fabrication processes as other thin-film solar cell materials. The multi-layer structure consists of a substrate (glass or metal foil) as a carrier, the back contact (molybdenum), absorber (*p*-conducting Cu(In,Ga)(S,Se)₂ for the absorption of the photons and the *n*-conducting transparent window (*n*-ZnO), which collects the electrons and leads them to the metal front contact grid.

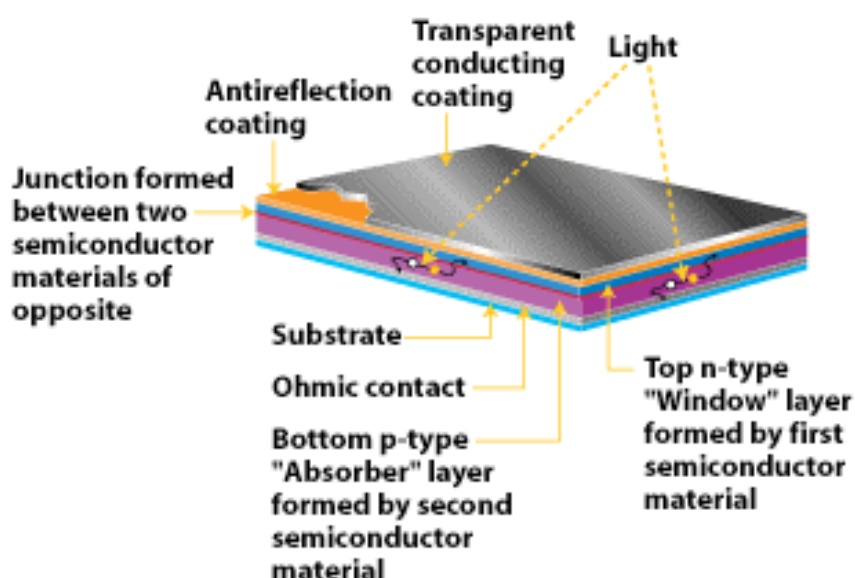


Figure 7. Polycrystalline thin-film cells have a heterojunction structure, in which the top and the bottom layer are made of different semiconductor materials. The top layer, usually *n*-type, is a window that allows almost all the light through to the absorbing layer, usually *p*-type. (EERE Information Center)

Typical solar cells are deposited on Mo-coated glass substrates at a substrate temperature above 500 °C. The heterojunction is formed by chemical deposition of a thin CdS layer from a solution containing Cd-ions and thiourea as a sulfur source. The most efficient devices and first large scale production of modules still rely on the CdS layer. However, research in many laboratories concentrates on the replacement of the CdS layer. Prospective materials for substitution of inorganic semiconductors in solar cells could be conductive polymers and photosensitive organic semiconductors [.,].

Table 1). One effort in Japan includes a wet deposited Zn(S,OH) compound already in pilot production [93]. Prospective materials for substitution of inorganic semiconductors in solar cells could be conductive polymers and photosensitive organic semiconductors [94,95,96].

Table 1. Summary of the best Cu(In,Ga)Se₂ -based solar cell efficiencies ($A \leq 1 \text{ cm}^2$) realised with different Cd-free buffer layer materials and deposited by different methods [97]

Material	Method	η (%)	Institute
CdS	CBD	19.2	NREL
ZnS-based	CBD	18.6	NREL/AGU
In(OH) ₃ -based	CBD	14.0	TIT
In ₂ S ₃ -based	CBD	15.7	IPE/ÅSC
	ALD	16.4	ENSCP/ZSW
ZnSe-based	CBD	15.7	HMI/Siemens
ZnInSe _x	Coevap.	15.3	TIT
ZnMgO	Sputtering	16.2	Matsushita Elec.
ZnO	Sputtering	15.0	NREL
SnO ₂	CBD	12.2 ^a	IPE

2. GOALS OF THE RESEARCH

The aims of the research are as follows:

- a. Investigation of the mechanism and kinetics of cathodic electrosynthesis of CuInSe₂
- b. Development of thin CuInSe₂ films with tailored composition and properties
- c. Development of methods of different thermal, chemical and electrochemical post-treatments of precursor films
- d. Preparation and investigation of PV structures on the base of the electrodeposited CuInSe₂ absorber

3. EXPERIMENTAL

3.1. VOLTAMMETRIC STUDY AND ELECTRODEPOSITION OF FILMS

Voltammetric measurements and electrochemical deposition were carried out using potentiostat Voltalab PGZ 100 with a conventional three-electrode cell. A saturated calomel electrode (SCE) or 3M Ag/AgCl electrode served as the reference electrode and Pt-foil was used as the counter electrode. Mo-covered or indium tin oxide (ITO) coated glasses were used as substrates and working electrodes.

Commercially available ITO/glass substrates with a surface sheet resistance of $< 20 \Omega/\text{cm}^2$ were used in our experiments. The Mo coated glass substrates were prepared by sputtering and they were typically $1\mu\text{m}$ thick and had sheet resistance of $0.2\text{-}0.3 \Omega/\text{cm}^2$. Before electrodeposition, the substrates were cleaned in hot (90°C) conc. H_2SO_4 for 1 minute.

All the experiments were carried out at room temperature. Aqueous solutions of 10mM selenious acid and 7-20mM indium and 1-10 copper sulfates were used as precursor solutions for CuInSe_2 film deposition. Potassium chloride acting as a complexing agent of metallic ions was used for the electrodeposition in concentrations 0-1 mol/l. The pH of electrochemical bath for deposition of thin films was in the region of 1-3. The deposition potential varied in the range -0.5 - -0.8 V vs. SCE. All the chemicals of an analytical grade (Merck) were dissolved in Millipore water (18 M Ohm cm).

Acidic 0.1M H_2SO_4 as well as basic 0.1 M NaOH electrolytes were used in the experiments of voltammetric and photo-voltammetric characterization of thin films. The scan rate varied between 5-20 V/s. A halogen lamp provided white illumination for photo-voltammetric measurements. The distance between the lamp and the working electrode was held at about 10 cm. A light chopping sequence of 0.5 s on and 0.5 s off was used.

3.2. POST-DEPOSITION TREATMENTS OF FILMS

A horizontal furnace was used for annealing the electrodeposited films either in H_2 or H_2S flow gas atmosphere, as well as for annealing in dynamic vacuum. The pressure at annealing in vacuum was 10^{-2} - 10^{-3} Torr. Samples were kept in a long quartz tube outside the furnace in the gas atmosphere and pushed inside the furnace in the heated zone. At the end of heat treatment, samples were pulled out and cooled down to the room temperature in the same gas atmosphere. Annealing in the atmosphere of Se vapour was provided in two-zone close ampoules. The used pressure of selenium vapour was 2 Torr at 500°C . The duration of post-treatments was from 15 min to 12 hours.

Different methods of etching were used to remove segregated phases from the surface of CuInSe_2 annealed films. The excess selenides of copper were removed by etching the films in an aqueous solution of 10 % KCN, 0.5%NaOH for 1min. Electrochemical etching was carried out or by potential scanning from -0.6 to $+0.6\text{V}$ at the scan rate of $10\text{mV}/\text{sec}$ in a 0.1

M H₂SO₄ solution or potentiostatically at +0.5V in a 0.1M NaOH solution. The hydroxides formed in the process of electrochemical etching in basic solutions were removed by short-time electrochemical etching in acidic solutions (1 min in solution of 0.1M H₂SO₄ at a -0.3 V).

3.3. CHARACTERIZATION OF FILM

Leo Supra 35 high resolution scanning electron microscope (SEM) was used to study the surface morphology of the deposited films. Chemical composition of the films was determined by energy dispersive X-ray spectroscopy (EDS, Röntex)). Optical transmission of the samples was measured by the UV-Vis spectrophotometer Shimadzu PC-2401. The phase composition of films was determined by X-ray diffraction analysis using Bruker AXS D5005 diffractometer with Cu K_α radiation.

3.4. PREPARATION OF SOLAR CELLS

The majority of the solar cell structures were prepared on the base of thin (about 500 nm) *n*-type CuInSe₂ films deposited by one step-electrodeposition (Articles [III](#),[IV](#), [V](#),[VI](#),[VII](#)).

The ITO/In(O,S)/CuIn(S,Se)₂ structures (see Articles [III](#),[IV](#)) were produced by the sulfurization of deposited ITO/CuInSe₂ precursor structures. The ITO/CuInSe₂ precursor structures were annealed in quartz tubes in H₂S flow at 450°C during 30 min for their sulfurization.

The ITO/In(O,S)/CuIn(S,Se)₂/PEDOT-PSS structures. A hybrid solar cell based on the combination of photoactive structure ITO/In(O,S)/CuInS_xSe_{2-x} and conductive polymer poly(3,4-ethylenedioxythiophene) (PEDOT) doped with polystyrenesulfonate (PSS), was obtained (Articles [IV](#)). The ITO/In(O,S)/CuInS_xSe_{2-x} structure was prepared as stated above. The PEDOT-PSS layer of *p*-type is considered an alternative to the traditional window top layer on the cell structure. The 1.3 wt. % aqueous dispersion of the conductive polymer PEDOT doped with PSS was purchased from Aldrich. 5 ml PEDOT-PSS aqueous dispersion was mixed with 120 μl glycerine, 250 μl N-methyl-2-pyrrolidone, 6.25 ml isopropanol and 81 μl tetraethoxysilane. Chemat Technology KW-4A precision spin-coater was used for deposition of polymer coatings with a thickness of about 50 nm. Gold was evaporated in vacuum onto the surface of the PEDOT-PSS films for the preparation of golden contact grids (Article [IV](#)).

The ITO/CuInSe₂/Polymer structures. Photovoltaic structure ITO/CuInSe₂/Polymer/Ag was fabricated in the sandwich configuration as shown in Figure 8.

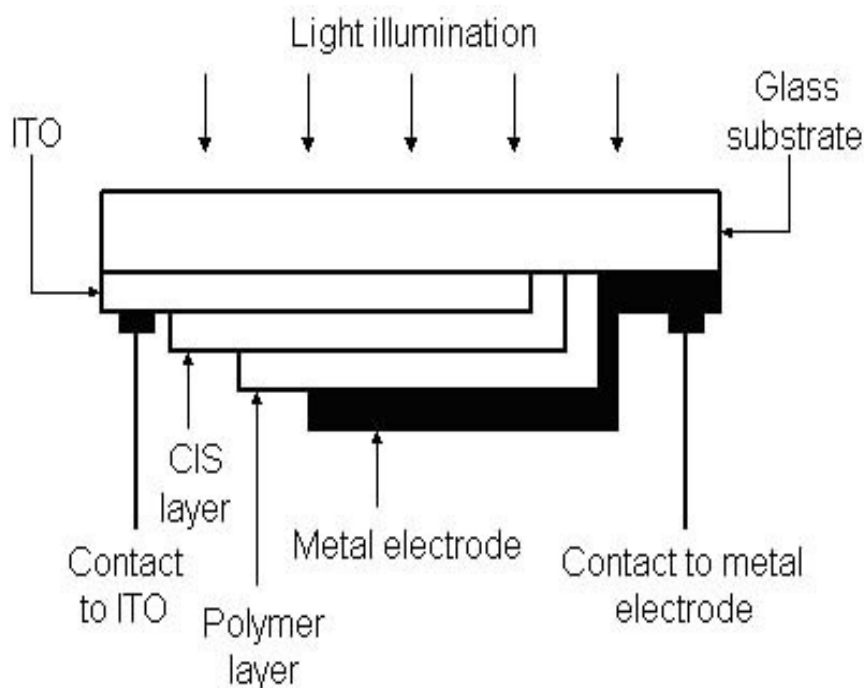


Figure 8. Schematic drawing of the ITO/CuInSe₂/Polymer/Ag photovoltaic structure

The *p*-type polymer layer of the polypyrrole (PPy) or polyaniline (PANI) covers the *n*-type CuInSe₂ films and forms an *n-p* junction. Conductive soluble PANI was chemically synthesized by the *in situ* doping oxidative polymerization of aniline at low temperature (0-2 °C). The p-PANI layer was cast onto the glass / ITO / *n*-CuInSe₂ substrate from PANI solution in chloroform (Article VII).

Doped PPy films with a thickness of about 1 μm onto the prepared glass/ITO/*n*-CISe substrates were synthesized galvanostatically between 0.55 and 0.65 V vs. SCE in a current density range from 0.25 to 0.5 mA/cm² (Article V). The doped PPy and PANI films were annealed at 100° C for 6 h in air whereas its adherence to the CuInSe₂ was markedly improved. Finally, metal strip electrodes (Ag) were evaporated onto the polymer layer.

Investigation of the prepared PV structures. The current-voltage measurements were performed using a KEITHLEY 2400 Source Meter. White light with an intensity of 100 mW/cm² from a tungsten-halogen lamp was used to measure current-voltage values. Impedance and current-voltage measurements were performed using an Autolab PGSTAT 30 potentiostat/galvanostat.

4. RESULTS

The main results of the author are summarized in this chapter. As results of research of morphology of the annealed films are published only partly yet, morphology of the annealed films is characterized here in more detail.

4.1. ELECTROCHEMICAL DEPOSITION OF CuInSe₂ FILMS

4.1.1. CHEMICAL PROCESSES IN AN ELECTROCHEMICAL BATH

The mechanism of electrodeposition of chalcopyrite films and the parameters of the obtained films are determined by the electrochemical behaviour of three constituent elements (Cu, In, Se). Each of these elements possesses specific electrochemical properties making the overall system very complex, even for the deposition of all three elements together in a single bath [1].

Indium (III) is known to be extensively hydrolyzed in aqueous solutions [98,99,100,101,102]. In order to minimize this effect, the electrolyte containing indium was prepared mainly on acidic solutions. In the presence of selenite species in a solution, indium is able to form stable complexes $\text{In}_2(\text{SeO}_3)_3 \cdot 6\text{H}_2\text{O}$ ($\text{pK}=32.6$) [103]. Stabilization time of the complexes is from several hours to several days [103].

Chloride ions added in plenty could replace the oxygen-containing species (SeO_3^{2-} or H_2O) [102] and form the stable soluble complexes of indium. The formed aquatic solution 5mM CuSO_4 , 10mM $\text{In}_2(\text{SO}_4)_3$, 10mM SeO_2 and 1M KCl remains stable during the months at $\text{pH} \approx 3$. Depending on the concentration of chloride ions in the solution and pH , various complexes of indium could be formed that include various neutral, anionic and cationic species [101]. The constitution of the electrolyte still requires optimization.

4.1.2. FILM GROWTH

4.1.2.1. THERMODYNAMIC ASPECT OF ELECTRODEPOSITION CuInSe₂ FILMS

The mechanism of CuInSe₂ formation through a number of consecutive reactions is presented in Figure 10 and described in Article I. The formation of the Cu + Se phases precedes the assimilation of indium and formation of the CuInSe₂ compound. The reactions of compound formation are displayed in Table 2.

The composition of electrodeposited copper selenides depends on the fluxes of the reactive species in the solution, i.e. on the transport phenomenon [17] and represents the mixture of pure components from Cu + Cu₂Se, CuSe+Cu₂Se to CuSe +Se. As the electrode potential is decreased further, CuSe is expected to change to Cu₂Se, and then Cu₂Se reduces to Cu⁰ and H₂Se, also Se⁰ reduces to H₂Se. The reaction of selenide ions with In(III) results in the formation of In₂Se₃ and later CuInSe₂ is formed by a subsequent reaction with Cu₂Se.

Table 2. Selected reactions in the Cu + In + Se+H₂O system

Reaction	
$\text{Se(IV)} + 4\text{e}^- \leftrightarrow \text{Se}^0$	1
$\text{Cu(II)} + \text{Se}^0 + 2\text{e}^- \leftrightarrow \text{CuSe}$	2a
$\text{Cu(II)} + \text{Se(IV)} + 6\text{e}^- \leftrightarrow \text{CuSe}$	2b
$\text{Cu(II)} + \text{CuSe} + 2\text{e}^- \leftrightarrow \text{Cu}_2\text{Se}$	3a
$2\text{Cu(II)} + \text{Se(IV)} + 8\text{e}^- \leftrightarrow \text{Cu}_2\text{Se}$	3b
$2\text{Cu(II)} + \text{Se}^0 + 4\text{e}^- \leftrightarrow \text{Cu}_2\text{Se}$	3c
$2\text{CuSe} + 2\text{e}^- \leftrightarrow \text{Cu}_2\text{Se} + \text{Se(II-)}$	4
$\text{Cu}_2\text{Se} + 2\text{e}^- \leftrightarrow 2\text{Cu}^0 + \text{Se(II-)}$	5
$\text{Se}^0 + 2\text{e}^- \leftrightarrow \text{Se(II-)}$	6
$2\text{In(III)} + 3\text{Se(IV)} + 18\text{e}^- \leftrightarrow \text{In}_2\text{Se}_3$	7a
$2\text{In(III)} + 3\text{Se}^0 + 6\text{e}^- \leftrightarrow \text{In}_2\text{Se}_3$	7b
$\text{In(III)} + \text{Cu(II)} + 2\text{Se(IV)} + 13\text{e}^- \leftrightarrow \text{CuInSe}_2$	8a
$\text{Cu(II)} + \text{In(III)} + 2\text{Se}^0 + 3\text{e}^- \leftrightarrow \text{CuInSe}_2$	8b
$2\text{In(III)} + 3\text{Se(II-)} \leftrightarrow \text{In}_2\text{Se}_3$	9
$\text{Cu(II)} + \text{Se(II-)} \leftrightarrow \text{CuSe}$	10
$\text{Se(IV)} + \text{Se(II-)} \leftrightarrow 2\text{Se}^0$	11
$\text{Cu}_2\text{Se} + \text{In}_2\text{Se}_3 \leftrightarrow 2\text{CuInSe}_2$	12
$\text{CuInSe}_2 + 4\text{e}^- \leftrightarrow \text{Cu}^0 + \text{In}^0 + 2\text{Se(II-)}$	
$\text{Se(IV)} + 6\text{e}^- \leftrightarrow \text{Se(II-)}$	14
$\text{In(III)} + 3\text{e}^- \leftrightarrow \text{In}^0$	15

Selenium can exist in the form of various phases due to existence of different (II), (IV) and (VI) oxidation states. It multiplies the number of reactions (redox couples).

Standard potentials at these oxidation states with different protonated forms have been calculated by the computer program HCS-4. The pH-E stability field diagrams were drawn for activities of reactive species 10^{-2} mol l⁻¹ in Figure 9. For simplicity and readability of data, the data of immunity, passivity and corrosion are considered only for stoichiometric (selected) elements.

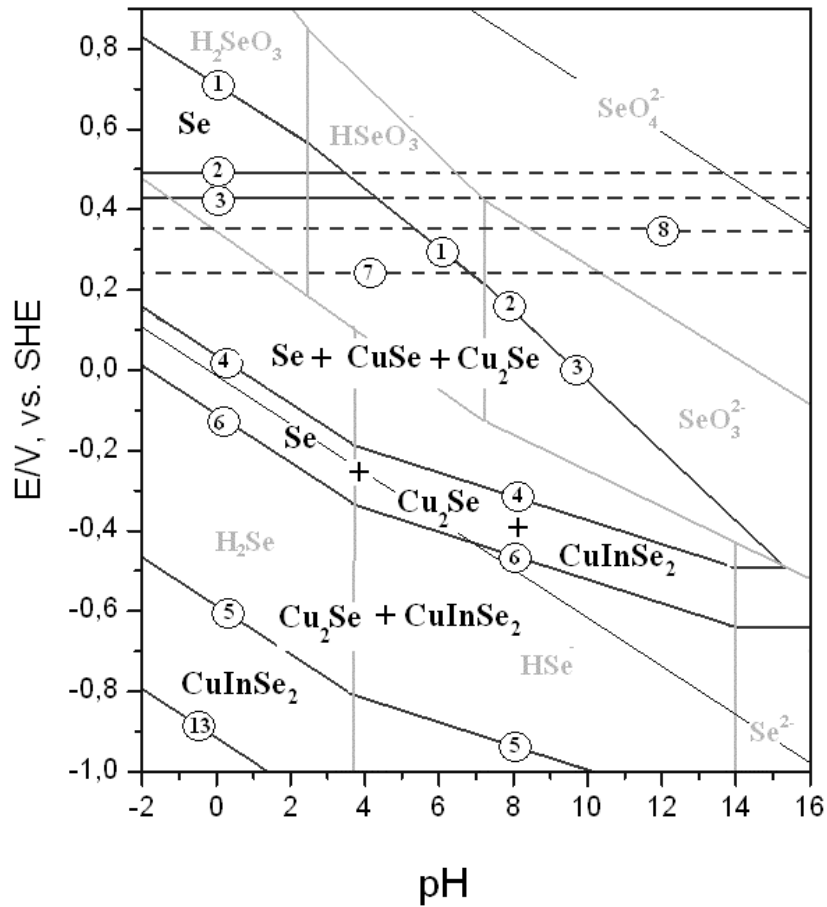


Figure 9. Pourbaix diagram for Cu+In+Se+H₂O system at 25°C. Candidate reactions for assembling this diagram are shown in Table 2.

It could be noted that the mechanism of CuInSe₂ formation is determined by the behaviour of selenium species (redox potentials). The insertion potential of copper depends on the redox potential Se(IV)/Se⁰ and the insertion potential of indium depends on the redox potential Se⁰/Se(II-).

Based on the above, the aim of the study was to verify the mentioned guidelines of underpotential deposition experimentally for the direct electrodeposition of thin films with various compositions in the Cu-In-Se system.

4.1.2.2 KINETIC ASPECT OF ELECTRODEPOSITION CuInSe₂ FILMS

The associated model used to determine the fluxes of copper, indium and selenium species to the cathode and relative concentrations of deposited solid phases is shown in Figure 10. This model is more advanced than that described in Article I.

Electrochemical reactions

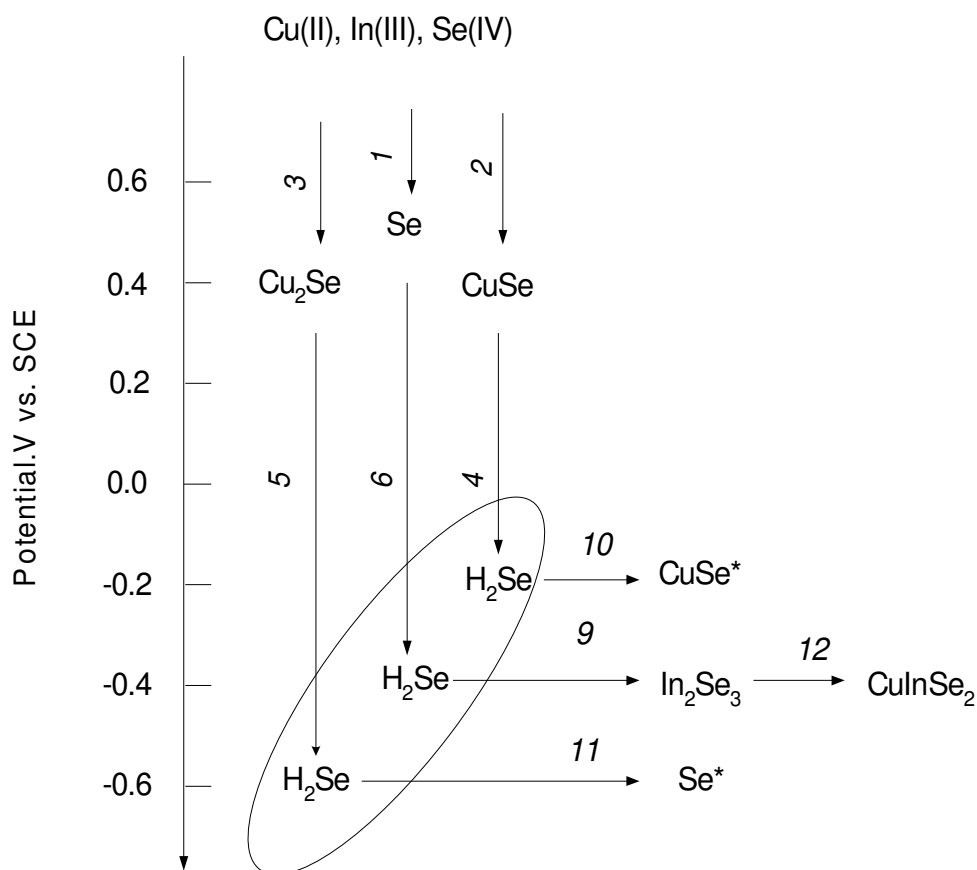


Figure 10. Simplified scheme showing the mechanism of formation compounds at electrochemical deposition of CuInSe₂

As soon as the process of underpotential deposition of CuInSe₂ is determined by the deposition of Cu + Se phases, the features of this process will be recalled first. Parallel reactions 1, 2 and 3 form Se⁰, CuSe and Cu₂Se phases. In the conditions of electrodeposition of CuInSe₂ films, the applied potential is much more negative than the potentials of formation of each of Cu + Se compounds. The reactions of the formation of Cu+Se phases are under kinetic control.

The reaction mechanism is derived by writing down the kinetic relations corresponding to each reaction partner. The deposition of Se(IV) in reasonable quantities is possible only if copper ions present in the solution accommodate Se in the deposit [37]. Thus, the deposition rate of CuSe could be presented as a second order reaction

$$\frac{d[\text{Cu}_2\text{Se}]}{dt} = \frac{1}{2}k_3 [\text{Cu(II)}]^{el}[\text{Se(IV)}]^{el} \text{ or } \frac{1}{2}k_3 [\text{Cu(II)}]^{el}[\text{Cu(II)}]^{el}, \quad \text{Eq.14}$$

where k_3 is the rate constant of reaction 3 (see Table 2).

At stationary conditions, the rate of deposition, $\frac{d[X]}{dt}$, is constant and it is possible to calculate the abundance of depositing phases Cu₂Se, CuSe and Se⁰ (see Table 3), where $J_{\text{Se(IV)}}$ and $J_{\text{Cu(II)}}$ fluxes of selenium and copper species are related to the concentrations in

the solutions by the expression given in Eq.8 and Eq.12. α , ratio $J_{Se(IV)}/J_{Cu(II)}$, is proportional to $[Se(IV)]/[Cu(II)]$

Under the conditions of diffusion limited current density j_{lim} the concentrations on the electrode are diminished and reached 0, $[X]^{el} = 0$. Using the fluxes of reacting species, the deposition rate could be described by

$$J_{Cu(II)}^{lim} = \frac{D_{Cu(II)}}{\delta_{Cu(II)}} [Cu(II)] = R_{Cu} [Cu(II)], \text{ then} \quad \text{Eq.15}$$

$$\frac{d[Cu_2Se]}{dt} = 1/2 k_3 R_{Cu}^2 [Cu(II)]^2 \quad \text{Eq.16}$$

$$R_{Cu} = \frac{D_{Cu(II)}^{lim}}{\delta_{Cu(II)}^{lim}} .$$

The reduction of Cu_2Se , $CuSe$ and Se^0 phases to H_2Se occurs at potentials -0.6, -0.2 and -0.4V vs. SCE in the acidic medium (pH \approx 1) and is controlled by thermodynamics. The rate of H_2Se formation could be calculated by

$$\frac{d[H_2Se]}{dt} = k_5^* [Cu_2Se] + k_6^* [Se^0] + k_4^* [CuSe], \quad \text{Eq.17}$$

where k_x^* is the rate constant of the reaction limited by thermodynamics, determined by Eq.7.

The rate of reactions 9, 10 and 11 (reactions of reduced H_2Se with species from the solution) are described by

$$\frac{d[In_2Se_3]}{dt} = 1/3 k_9 [H_2Se] [In(III)]^{el} \quad \text{Eq.18}$$

$$\frac{d[Se^*]}{dt} = 2k_{11} [H_2Se] [Se(IV)]^{el} \quad \text{Eq. 19}$$

$$\frac{d[CuSe^*]}{dt} = k_{10} [H_2Se] [Cu(II)]^{el} \quad \text{Eq. 20}$$

Now it is possible to calculate the fraction of each formed solid product for each composition of the solution and each potential value. Table 3 presents the rate of the formation of components (including intermediate products) as functions of fluxes of reagent species.

In the calculation of copper and selenium fluxes we have to determine concentrations of reagent species at the surface of the electrode $[X]^{el}$ and in the bulk $[X]$ that makes calculations very complicated. In the conditions of current-controlled diffusion, where $[X]^{el} = 0$, the abundance of each compound is a function of the concentration of reacting species in the solution and the applied potential calculated by formulae given in Table 3

Table 3. Rate of formation of the compounds and elemental composition of deposited films as the function of the fluxes of reagent species

Rate of formation compounds	$d[X]/dt$	$d[X]/dt$ <i>lim current</i>
$d[Cu_2Se]/dt$	$1/2 k_3 [Cu(II)]^{el} [Cu(III)]^{el}$	$1/2 k_3 R_{Cu}^2 [Cu(II)]^2$
$d[CuSe]/dt$	$J_{Cu(II)} - 2 d[Cu_2Se]/dt$	$R_{Cu} [Cu(II)] - k_3 R_{Cu}^2 [Cu(II)]^2$
$d[Se]/dt$	$J_{Se(IV)} - d[CuSe]/dt - d[Cu_2Se]/dt$	$R_{Cu} [Cu(II)] (\alpha - 1 - 1/2 k_3 R_{Cu} [Cu(II)])$
$d[H_2Se]/dt$	$k_5^* [Cu_2Se] + k_6^* [Se^0] + k_4^* [CuSe]$	$k_5^* [Cu_2Se] + k_6^* [Se^0] + k_4^* [CuSe]$
$d[In_2Se_3]/dt$	$1/3 k_9 [H_2Se] [In(III)]^{el}$	$1/3 k_9 [H_2Se] [In(III)]$
$d[CuSe]^*/dt$	$k_{10} [H_2Se] [Cu(II)]^{el}$	0
$d[Se]^*/d$	$2 k_{11} [H_2Se] [Se(IV)]^{el}$	0
Abundance of species in the deposited film, at. %	$[x]/[dep]$	$[x]/[dep]$ <i>Limiting current</i>
Cu	$J_{Cu(II)}$ $2/3 k_9 [H_2Se] [In(III)]^{el} + J_{Cu(II)} + J_{Se(IV)}$	$K_{Cu(II)} [Cu(II)]$ $2/3 K_{In(III)} [H_2Se] [In(III)] + (1 + \alpha) K_{Cu(II)} [Cu(II)]$
In	$2/3 k_9 [H_2Se] [In(III)]^{el}$ $2/3 k_9 [H_2Se] [In(III)]^{el} + J_{Cu(II)} + J_{Se(IV)}$	$2/3 K_{In(III)} [H_2Se] [In(III)]$ $2/3 K_{In(III)} [H_2Se] [In(III)] + (1 + \alpha) K_{Cu(II)} [Cu(II)]$
Se	$J_{Se(IV)}$ $2/3 k_9 [H_2Se] [In(III)]^{el} + J_{Cu(II)} + J_{Se(IV)}$	$\alpha K_{Cu} [Cu(II)]$ $2/3 K_{In(III)} [H_2Se] [In(III)] + (1 + \alpha) K_{Cu(II)} [Cu(II)]$

The results of computation enable us to draw up the distribution diagram of the final products. Figure 11 presents the composition of films deposited under diffusion limited current conditions. Experimental data are marked by points and continuous theoretical curve is calculated. The distribution triangle diagram of elements in the deposit, in depending on the composition of electrolyte and the deposition potential is shown in Figure 12.

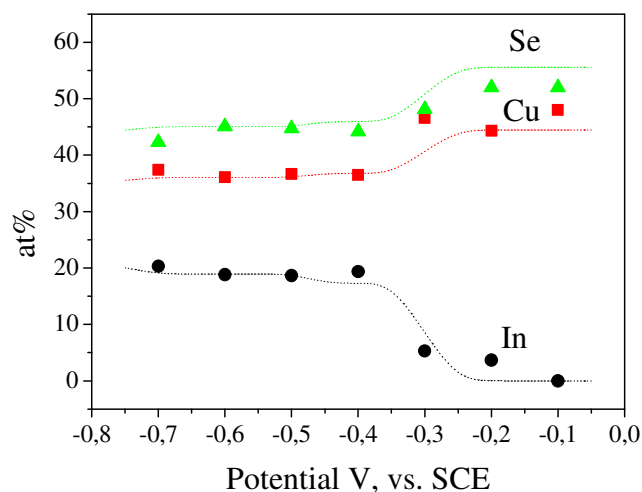


Figure 11. Comparison between the calculated and the observed variation of composition with deposition potential. Films were obtained from 10mM CuCl_2 , 5mM In_2Cl_3 and 10mM SeO_2 solution, pH= 2. Dotted lines represent the calculated composition

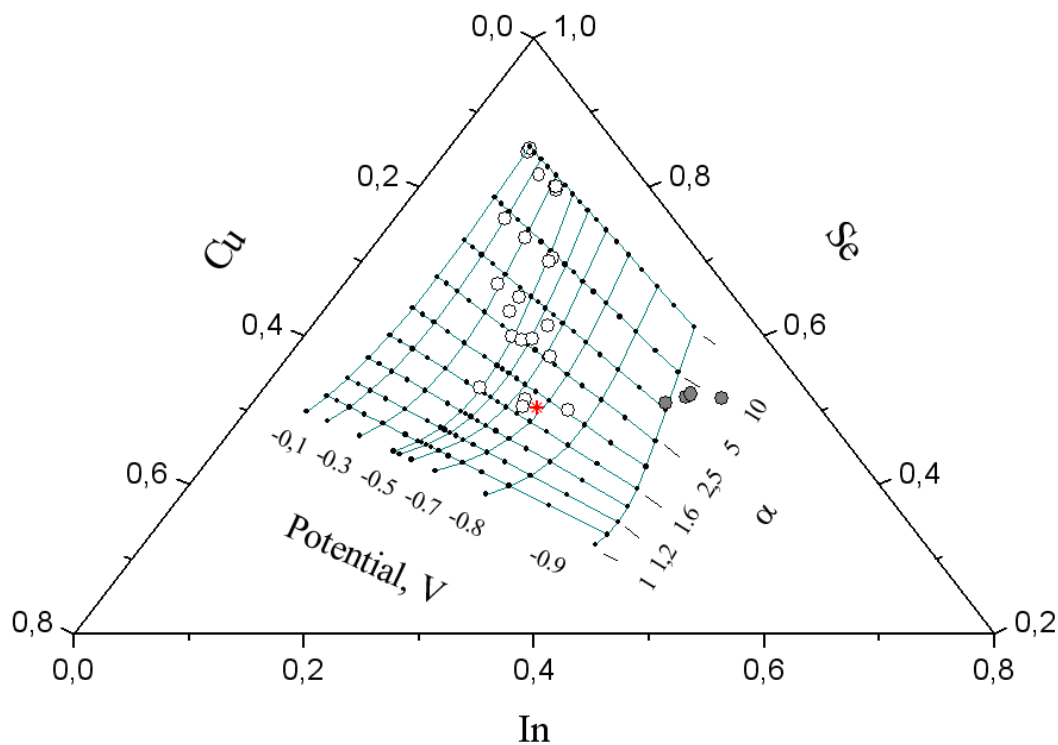


Figure 12 The calculated distribution diagram of elements in the deposit, in depending on the composition of electrolyte and the deposition potential. Experimental data are marked by white points (Table 4) and black points (Table 5), * is CuInSe_2

The deposition of a stoichiometric CuInSe₂ thin film was provided from acidic solution at potentials -0.5 –0.7V vs. SCE. The electrochemical bath contained copper and selenium species in the ratio 1:2 and indium ions in abundance. The typical solution was 5mM CuCl₂, 5mM In₂Cl₃ and 10mMSeO₂, pH= 2. 1M solution KCl was used to stabilize the solution (Section 4.1.1). The composition of electrodeposited films is shown on Table 4, (Article I).

Table 4. The chemical composition of as-deposited CuInSe₂ films

Potential vs. SCE (V)	Composition of electrolyte, mM											
	Cu,%	In,%	Se,%	Cu,%	In,%	Se,%	Cu,%	In,%	Se,%	Cu,%	In,%	Se,%
	1	10	10	3	10	10	7	10	10	10	10	10
	Composition of the deposited thin films, at%											
-0,1	16.35	0	83.65	22.29	0	77.71	40.74	0	59.26	49.14	0	50.87
-0,2	9.38	1	89.62	22.98	2.8	74.22	35.89	4.36	59.75	39.73	12.55	48.72
-0,3	8.63	1.52	89.86	17.79	12.75	69.44	31.01	18.21	50.79	35.11	19.97	47.72
-0,4	6.79	5.18	88.03	18.11	16.85	65.03	28.73	21.5	49.77	37.35	16.82	43.83
-0,5	-	-	-	17.79	18.21	63.99	28.14	24.29	47.57	36.14	20.49	43.37
-0,6	-	-	-	17.48	27.53	54.99	-	-	-	-	-	-
-0,65	-	-	-	12.63	42.51	44.56	-	-	-	-	-	-

Electrochemically deposited thin films with excess of indium were used as n-type absorber films. (Article V) The films have a large deviation from stoichiometric CuInSe₂, and after thermal treatment could be considered as films of ordered vacancy compounds CuIn₂Se_{3,5}, CuIn₃Se₅ [104]. The composition of these thin films is controlled via the composition of electrolytes (Table 5).

Table 5. Composition of thin films electrodeposited from solutions of different composition

Composition of electrolyte mM			Potential, mV vs. SCE	Composition of films , at%		
Cu(II)	In(III)	Se(IV)		Cu(at%)	In(at%)	Se(at%)
2	8	11	-900	7.9	40.5	51.6
3	7	11	-900	10.9	37.3	51.8
4	6	110	-900	13.1	36.0	50.9
5	8	10	-900	22	28	50

Figure 13 presents typical X-ray diffractograms of as-deposited specimens obtained at various cathodic potentials. For the specimen deposited at 0V, peaks were identified as CuSe and Cu₂Se (Cu₃Se₂) phases. The intensities of these peaks decreased with increasing cathodic polarization and three peaks of CuInSe₂ were observed at $d= 0.332, 0.203$ and 0.174 nm. It is impossible to determine whether these peaks should be ascribed to chalcopyrite or spalerite phases because both structures [46] have diffraction peaks nearly the same location. Weak peaks characteristic only of the chalcopyrite structure were not detected in X-ray diffractograms. The absence of these peaks could be explained by poor crystallinity of as-deposited samples [105].

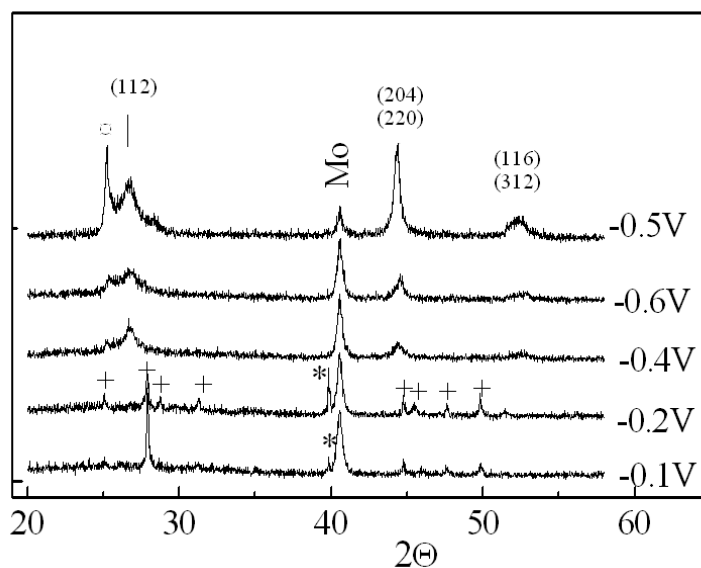


Figure 13. Diffraction patterns of films electrodeposited from the initial solution of 7 mM CuSO_4 , 5 mM $\text{In}_2(\text{SO}_4)_3$ and 10 mM SeO_2 , deposition time - 20 minutes (except -0.5 V , deposited for 60 min): + Cu_3Se_2 , * - undetermined peak, α - Cu_2Se

4.1.3. MORPHOLOGY OF DEPOSITED FILMS

The morphology of deposited films is described in Article I. The morphology of films is determined by the nucleation rate of crystals (is the function of overpotential) and the rate of mass transport of solute species. The nucleation rate of copper selenides establishes the morphology of CuInSe_2 at all. As the electrodeposition of CuInSe_2 can occur at potentials -0.4 V vs. SCE, an initial formation of copper selenides occurs under substantial overpotential (deposition potential $\text{CuSe} + 0.5\text{ V}$ vs. SCE).

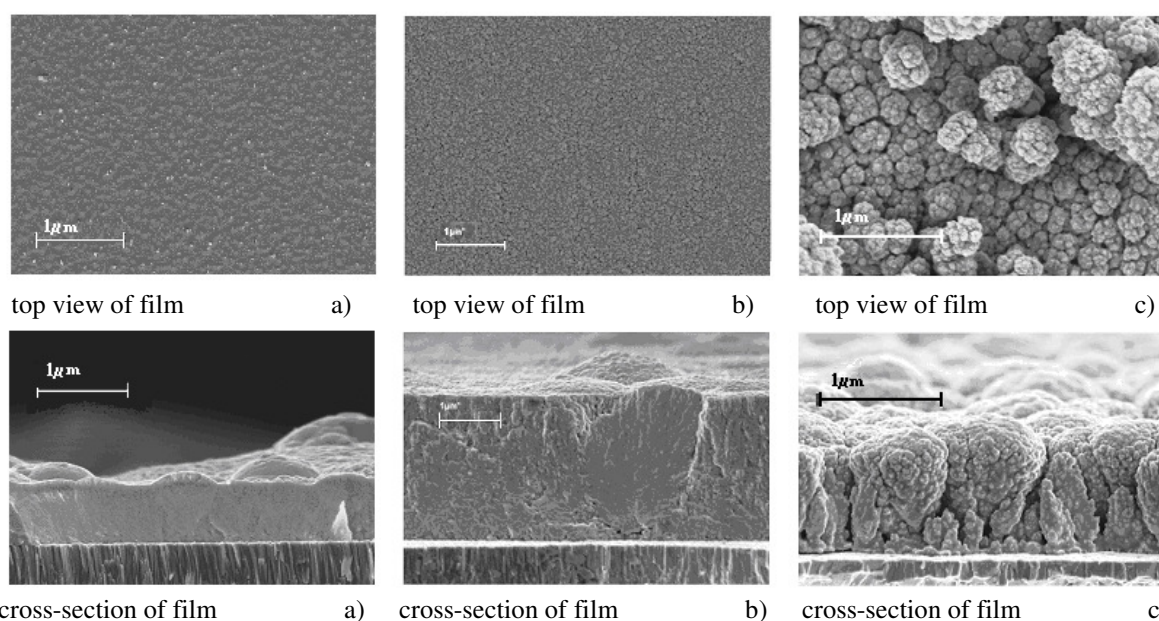


Figure 14. CuInSe_2 thin films obtained from solution 5mM CuSO_4 , 10mM $\text{In}_2(\text{SO}_4)_3$ and 10 mM SeO_2 at potential -600 mV vs. SCE.

Dense, smooth films were obtained, when the rate of deposition was not limited by the diffusion of reacting species (Figure 14 a). The CuInSe_2 films formed under the conditions of the limiting diffusion current density were of dendritic, porous structure (Figure 14 b and c). All the films shown in Figure 14 were deposited in the same conditions (but in different days) from solutions containing 5mM CuSO_4 , 10mM $\text{In}_2(\text{SO}_4)_3$ and 10 mM SeO_2 at potentials of -600 mV vs. vs. SCE. Differences in morphology could be explained by the instability of electrolyte (see section 4.1.1). At the same time, the composition of all these CuInSe_2 films was nearly stoichiometric.

The shape of dendrite like formations depends on the electrodeposition potential (overpotential). At higher overpotentials (-800V) and at larger values of current densities, porous and very disperse copper deposits were obtained. Figure 15 b. Powder-like deposits were formed at high potential (-1000mv and higher) where growth of CuInSe_2 films was accompanied with hydrogen evolution Figure 15 c.

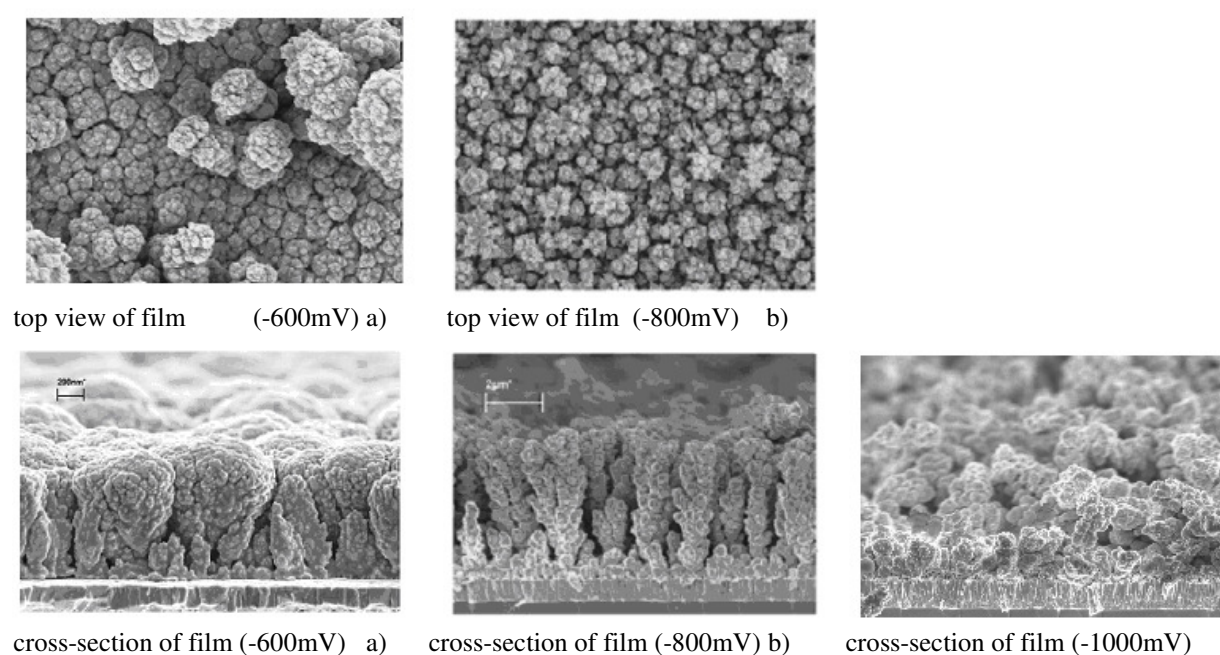


Figure 15. CuInSe_2 thin films obtained from solution 5mM CuSO_4 , 10mM $\text{In}_2(\text{SO}_4)_3$ and 10 mM SeO_2 at different cathodic potential.

The morphology of a film is independent of their summary composition that was discussed in (Section 4.1.2.2). Nevertheless, dense, smooth films were obtained in the conditions of the rate of deposition not limited by the diffusion reacting species, containing commonly the excess of Cu_2Se phases.

4.2. POST-DEPOSITION TREATMENT

4.2.1. ANNEALING UNDER Se VAPOUR PRESSURE

The results have not been published yet. A paper will be prepared on the basis of the thesis and will be proposed for publication soon.

In order to achieve the desired semi-conducting properties, the precursor films need to be thermally annealed. The morphology of annealed films and their optical and electrical properties are strongly dependent on the conditions of annealing (temperature, time and atmosphere of annealing).

Figure 16 shows the representative SEM micrographs of CuInSe₂ thin films, prepared by thermal annealing of electrodeposited precursors. The films were electroplated onto soda-lime glass covered by Mo at the potential -600 mV from 5mM CuSO₄, 10mM In₂(SO₄)₃, 10mM SeO₂ and 1MKCl. The average composition of the precursor film was 25at % Cu, 25at % In and 50at % Se. The annealing was done in different atmospheres (in vacuum, in Se vapour pressure) during 15 min at 500°C. The topographical images (the left column) and compositional contrast images (the right column) of the as-deposited film (Figure 18a) and of those annealed in different atmospheres are given (Figure 18b, c).

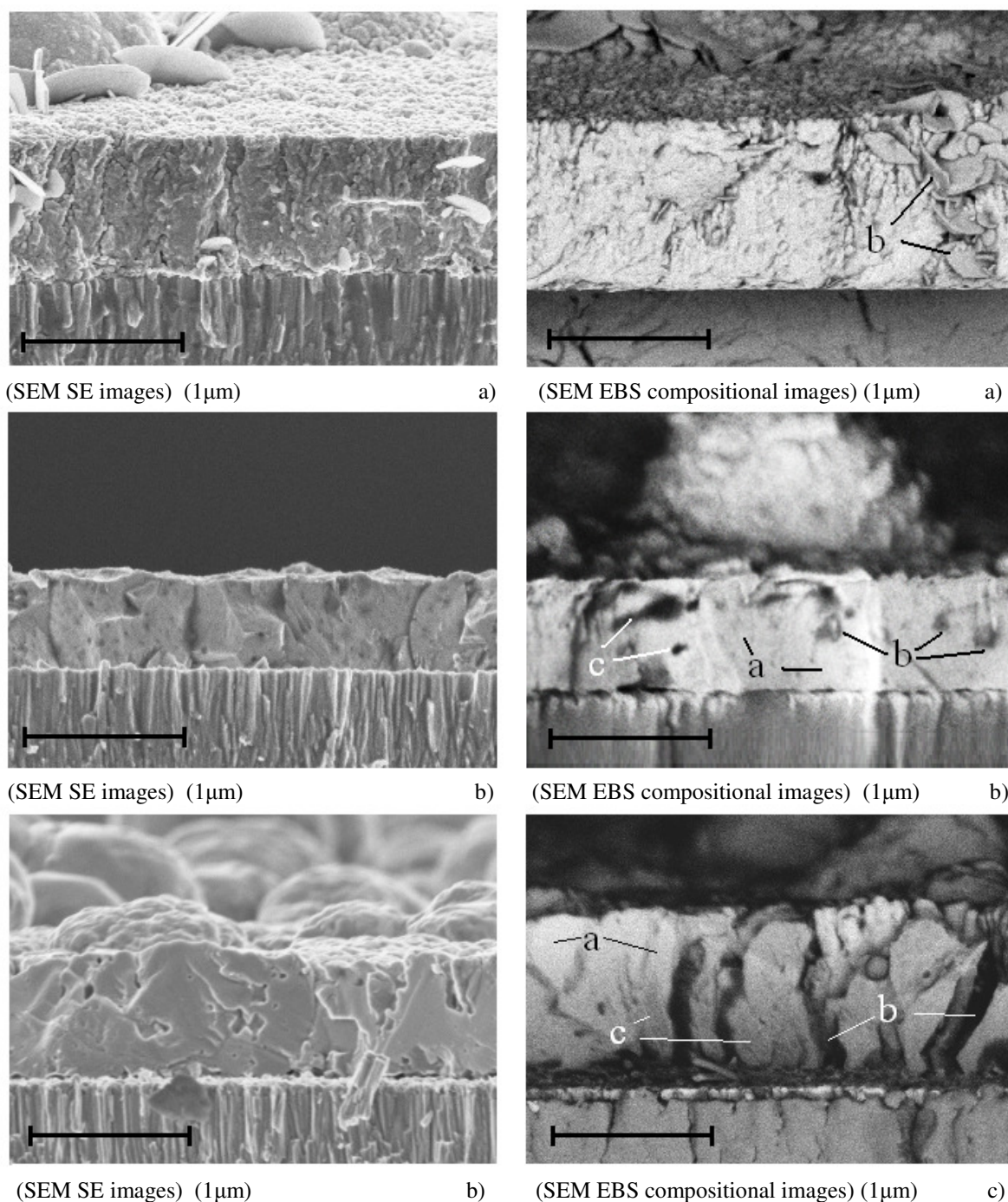


Figure 16 SEM images of cross-section of thin films a) non annealed, b) annealed in vacuum (10^{-3} Torr), c) annealed in selenium atmosphere (2 Torr) at 510°C during 15 min.

The structure of films annealed in vacuum (at equilibrium Se pressure of dissociation of CuInSe_2 is 10^{-3} Torr) is more dense, uniform and nanocrystalline as compared with all other films. The SEM EBS images expose the non-homogeneous structure with fragmentary inclusion of Cu-rich phases different by size and composition (see Figure 16b zone a and c). During annealing thickness of the films was reduced by up to one third (initial thickness of films was $1.5 \mu\text{m}$) due to an increase in the density of the reacted film and, perhaps, as a result of some loss of material during the annealing process. The dependence of morphology and composition of films on the duration of annealing is described below.

The basic microstructure of a film annealed under Se vapour pressure about 2 Torr is complex, with a range of planar defects: faceted voids, pores and variation in grain size. The grain size of crystals that form the CuInSe_2 thin-films is in the range of $1\text{--}1.5 \mu\text{m}$ and after selenization a single grain extends usually through the whole film thickness. The SEM EBS images reveal that the intergranular cracks are filled with secondary phases of copper selenides. Moreover, the composition gradient is clearly visible in the single crystallite (see Figure 16c, zone a and b)

The structure and morphology of the CuInSe_2 thin films have been found to be dependent on precursor composition and Se vapour pressure. The changes in magnitude of Se vapour pressure lead to changes in the relative kinetics of CuInSe_2 formation due to the modification of the availability of reactive Se species. High reactor pressure inhibits the formation of Se-rich binary compounds, which at $500 \text{ }^\circ\text{C}$ are believed to be in a quasi-liquid state and to provide high diffusion of reactive compounds [106].

4.2.2. THERMAL ANNEALING IN THE ATMOSPHERE OF H₂S

The influence of annealing electrodeposited precursor films in H₂S flow gas at 450°C during 30 min was described in detail in Articles III,IV. H₂S reacts at high temperature with material of as-deposited CuInSe₂ precursor film and as result CuIn(S_xSe_{1-x})₂ forms. Thus, the formation on indiumoxysulfide, In(O,S), nano-size films accompanies the formation of CuIn(S_xSe_{1-x})₂.as a result of diffusion of sulfur through thin films of formed CuIn(S_xSe_{1-x})₂ and reaction of sulphur with surface of ITO-conductive electrode.

Post-annealing of electrodeposited CuInSe₂ thin films in the flow of H₂S improves the films crystallinity as shown on the X-ray diffractogram in Figure 17.The size of the grains in CuIn(S,Se)₂ layer is in range of 200–250 nm. EDS analysis indicates to the loss of In from electrodeposited films in the annealing process and to a rise of sulfur content in films: the Cu:In:Se elemental ratio (in atom percent) in un-annealed films is 15:36:49, whereas in a film annealed in H₂S, the Cu:In:S:Se elemental ratio is 21:27:32:20.

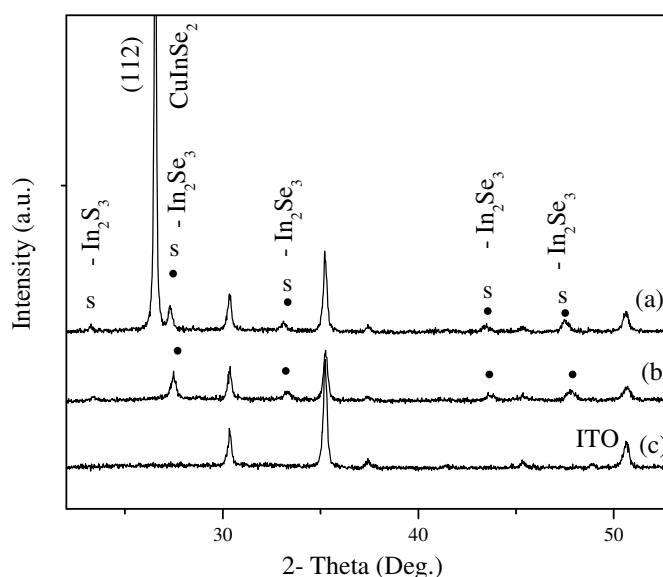


Figure 17. The XRD spectra of: a) annealed in H₂S and etched in 5% KCN; b) as-deposited CuInSe₂ thin films; c) ITO substrates

4.2.3. CHEMICAL AND ELECTROCHEMICAL ETCHINGS

Chemical etching in 0.5 %KCN, 0.05 %NaOH was carried out for removing Cu₂Se phases from the surface of films (Figure 18 b). The duration of etching was about 1 min. The composition of etched thin CuInSe₂ films was nearly stoichiometric, although the composition of annealed films was Cu-rich (see Table 6) (Article II).

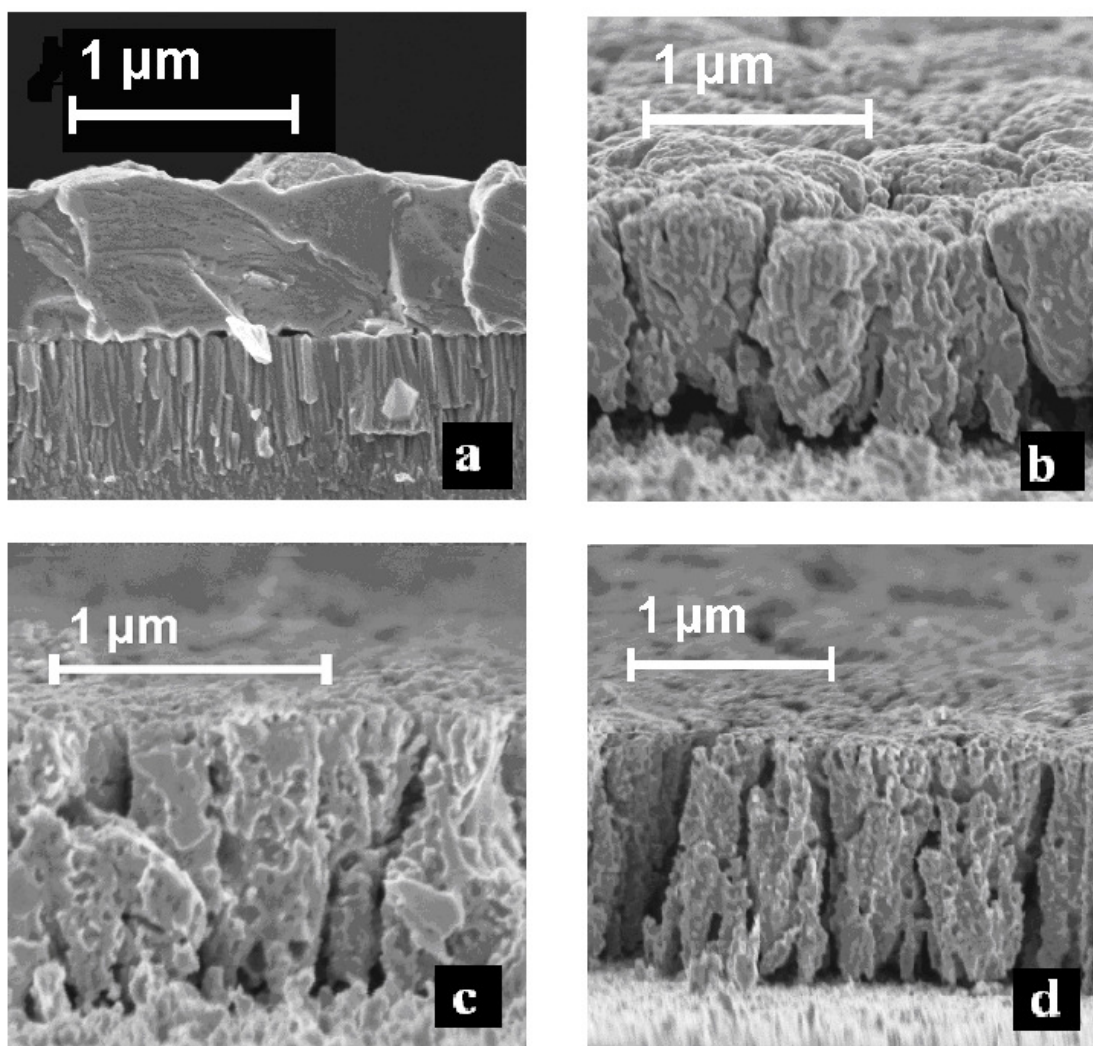


Figure 18. SEM cross-section of CInSe films: a) un-etched, b) etched in 5% KCN, c) electroetched in 0.1M H_2SO_4 , d) electroetched in 0.1M NaOH

The technique and results of electroetching of the Cu_{2-x}Se phase from the surface of CuInSe_2 films are described in detail in Article II. The electrochemical etching of the Cu_{2-x}Se phase from the surface of CuInSe_2 films is based on the difference of redox potential CuInSe_2 and Cu_{2-x}Se compounds in the acidic and alkaline medium. Based on the pH-E diagram (Figure 9) two methods of electrochemical etching were developed.

The first method is based on alternate removing of Cu_{2-x}Se by alternate reduction and oxidation at voltage scanning from -0.5 V to +0.5 V vs. SCE in an acidic electrolyte. The passivation effect is responsible for reduction current and the delay of the etching process. At reverse potentials, the surface reactivates. To summarize the above-given, Cu_{2-x}Se could be removed in an acidic electrolyte only by multiple scanning processes from negative to positive vs. SCE potentials.

The second method is based on the anodic oxidation of Cu_{2-x}Se phases at the potentiostatic regime +0.5V vs. SCE in basic solutions during 3 min. The final composition for all etched films was similar, corresponding to the stoichiometric composition of CuInSe_2 (Table 6). As an advantage, electrochemical etching removes Cu_2Se phases not only from the surface but

even from the intergrain areas. At the same time it could result in the formation of deep cracks through the films grown in “huge” excess of Cu in the electrodeposition solution (Figure 18).

Table 6. Composition of annealed and etched by different methods films

Etching	Cu at%	In at%	Se at%
Annealed	28.6	25	46.4
Etched in 5%KCN	23.9	27.3	48.8
Electrochemically in 0.1M H ₂ SO ₄	23.7	26.4	49.9
Electrochemically in 0.1M NaOH	25	25	50

4.3. CHARACTERIZATION OF THIN FILMS

The as-deposited layers have significant deviation from the stoichiometrical composition. Deviation from the stoichiometrical composition is the result of multiphase composition of as-deposited layers in nature. The layers consist of the CuInSe₂ phase together with separate phases of selenium and copper selenides in a proportion that depends on the deposition potential.

The absorption coefficient was calculated and was used to characterize optical properties of the films (Article III). Band gap energy (E_g) was determined from absorption curves by extrapolation $(\alpha h\nu)^2$ vs. $h\nu$ [107]. As-deposited CuInSe₂ thin films showed bandgap energies in the range 0.8-1.1 eV in dependence of their composition. The as-deposited Cu-rich film with virtual summary composition 24 at % Cu, 24 at % In and 52 at % Se has the value of $E_g = 0.87$ eV (Article II), the film with virtual elemental composition 11 at % Cu, 37 at % In and 52 at % Se has the value of $E_g = 1.0$ eV (Article IV, Figure 19).

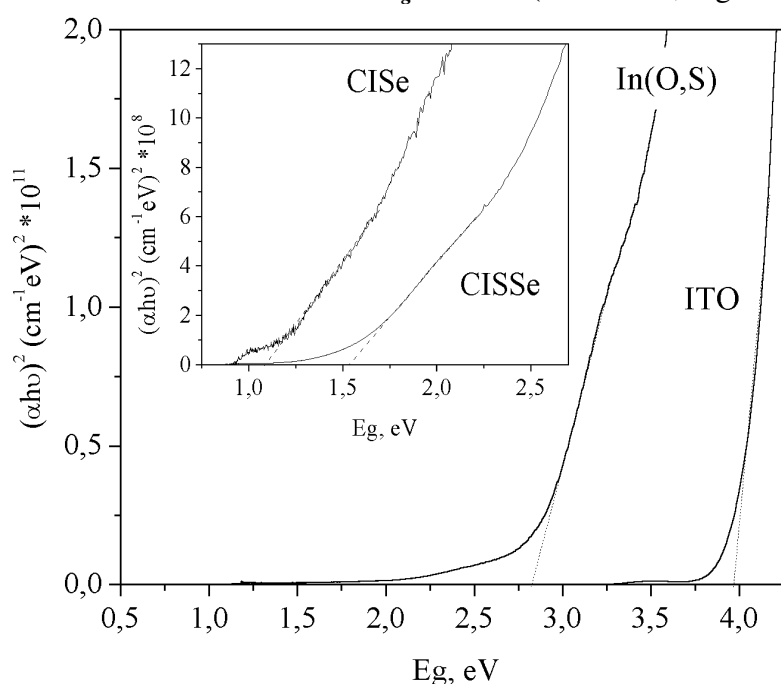


Figure 19. The plot of $(\alpha h\nu)^2$ against the photon energy $h\nu$. CISe is electrodeposited CuInSe₂, CISSe is sulfurized in H₂S CuIn(S,Se)₂ film.

Optical properties of electrodeposited CuInSe_2 films annealed in the atmosphere of H_2S are discussed in Article IV. It was found that the treatment in flowing H_2S at 450°C results in the increase of the bandgap up to 1.5eV .

Photoelectrochemical measurements were conducted to determine the type of conductivity of the prepared film. The typical dependence of photocurrent versus electrode potential for the n -type CuInSe_2 film under periodic illumination in a three-electrode cell in 0.1 M sulfuric acid solution is shown in Figure 20. The increase of the anodic current under illumination corresponds to the acceleration of oxidation reaction on the n -type electrode [108,109].

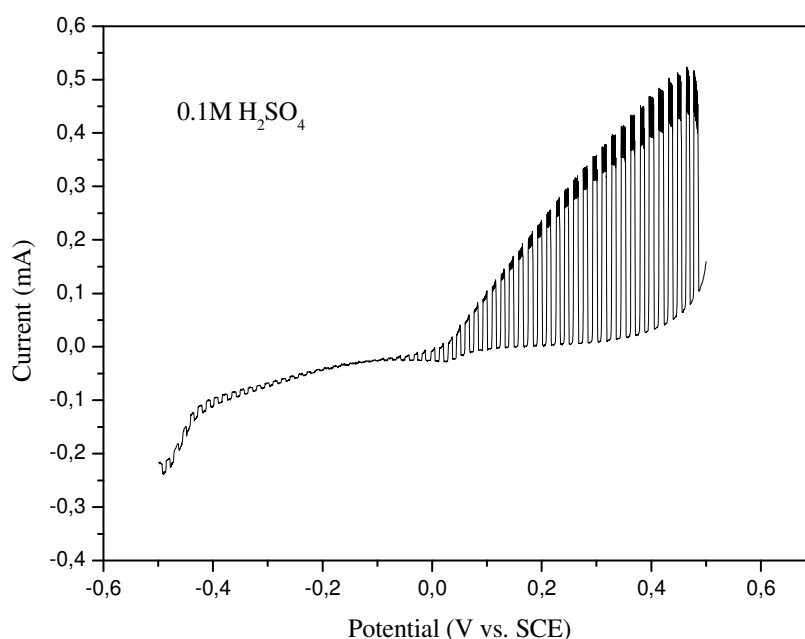


Figure 20. Current-potential curves of n -type CuInSe_2 film annealed in vacuum under periodic illumination. (Electrolyte $0.1\text{M H}_2\text{SO}_4$) $20\text{mV}/\text{sec}$

p -type semiconductor has a typical increasing current in the cathodic potential under illumination (see Figure 21) (Article II).

Article II presents the results of the photoelectrochemical characterization of CuInSe_2 post treated films. The results indicate to the remarkable effect of post-deposition treatments on photoactivities of films. Thus, for example, as-deposited and annealed films were very slightly photoactive (curve a). The film etched in the basic solution (curve d) has low photosensitivity due to the passivation of the surface by hydroxides. Short-time etching in the acidic solution restores the surface of CuInSe_2 films, leading to higher photoresponse (curve e)

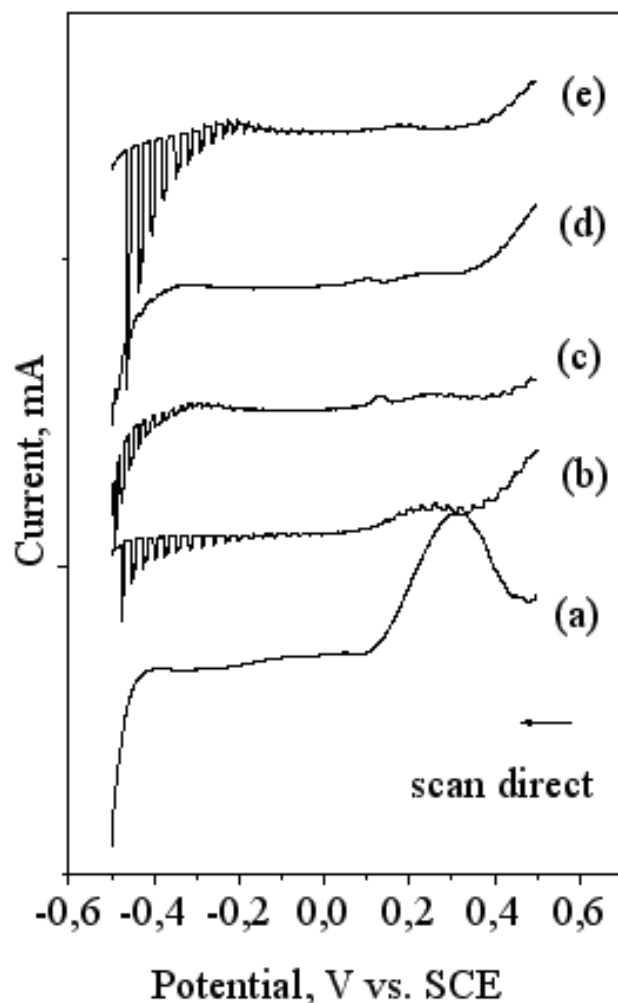


Figure 21. Photovoltammograms of films treated by various methods of etching: a) un-etched CuInSe_2 film, b) etched in 5% KCN, c) electroetched in 0.1M H_2SO_4 , d) electro-etched in 0.1M NaOH, e) electroetched in 0.1M NaOH and additionally electro-etched in an acidic solution (1 min at -0.3V in 0.1M H_2SO_4) (e). The active area of films was 1 cm^2 and scan rate was 10mV/ sec.

4.4. SOLAR CELL STRUCTURES ON ELECTRODEPOSITED CuInSe_2 FILMS

This thesis provides results of two types of solar cells prepared using electrochemically deposited precursor CuInSe_2 thin films: the Cd-free photovoltaic structure on the base of $n\text{-In(O,S)/p-CuIn(S,Se)}_2$ junction (Articles III and IV), and combined inorganic/organic $n\text{-CuInSe}_2/p\text{-polymer}$ photovoltaic structure (Articles V, VI and VII).

4.4.1. ITO/ $\text{In(O,S)/CuIn(S,Se)}_2$ PHOTOVOLTAIC STRUCTURE

The Cd-free superstrate photovoltaic structure was developed and investigated (Articles III and IV). The formation of an n -type In(O,S) buffer layer accompanies the synthesis of p -type CuIn(S,Se)_2 during the sulfurization of an electrodeposited CuInSe_2 layer. Sulfur

diffuses through the thin film of $\text{CuIn}(\text{S},\text{Se})_2$, reacts with the surface of ITO and forms $\text{In}(\text{O},\text{S})$. The presence of sulfur in an annealed ITO conductive film was confirmed by the results of EDS analysis of the $\text{In}(\text{O},\text{S})$ film surface from where $\text{CuIn}(\text{S},\text{Se})_2$ was removed. The change in the optical properties of ITO films after heat treatment in H_2S is shown in Figure 19. The formed $\text{In}(\text{O},\text{S})$ layer has direct band structure with bandgap 2.76 eV [97].

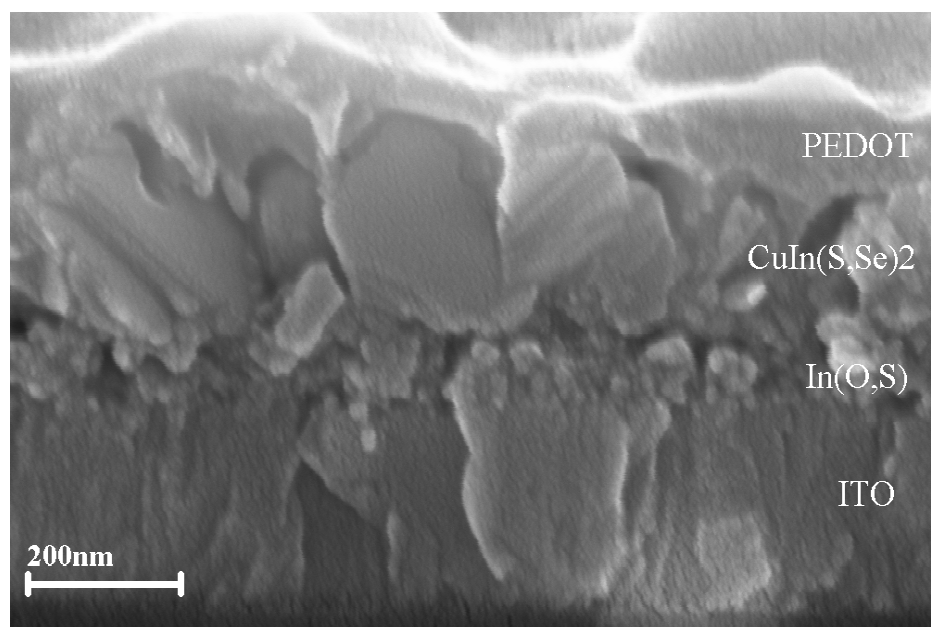


Figure 22 Cross-section of $\text{In}(\text{O},\text{S})/\text{CuIn}(\text{S},\text{Se})_2/\text{organic}$ photovoltaic structure

This fine-grained $\text{In}(\text{O},\text{S})$ buffer layer and the crystalline $\text{CuIn}(\text{S}_x\text{Se}_{1-x})_2$ absorber layer are shown in the cross-sectional SEM micrograph in Figure 22. The solar cell structures were completed by plating graphite back contact or organic windows layer with Au-grid. The active area of the $\text{ITO}/\text{In}(\text{O},\text{S})/\text{CuIn}(\text{S}_x\text{Se}_{1-x})_2/\text{graphite}$ structures was about 1 mm^2 . The electrical parameters of those structures depend on the condition of electrodeposition of precursor $\text{ITO}/\text{CuInSe}_2$ layers (Table 7). For the cells based on the CuInSe_2 films treated with H_2S , the highest open circuit voltage (V_{oc}) was 373 mV, whereas the short circuit current density (I_{sc}) was $1\text{ mA}/\text{cm}^2$ and the fill factor (FF) $\sim 25\%$.

Table 7. Performance of the $\text{In}(\text{O},\text{S})/\text{CuIn}(\text{S}_x\text{Se}_{1-x})_2$ cells produced by various post-fabricating treatments

Composition of electrolyte $\text{Cu}^{2+}/\text{In}^{3+}/\text{Se}^{4+}$ mM	1st annealing in H_2S			etching in 5% KCN			2nd annealing in H_2		
	I_{sc} mA/cm^2	V_{oc} mV	FF %	I_{sc} mA/cm^2	V_{oc} mV	FF %	I_{sc} mA/cm^2	V_{oc} mV	FF %
2/7/11	-1.0	297	25.2	-2.7	271	24.1	-2.0	289	27.2
3/7/11	-3.7	269	27.8	-5.7	301	28.1	-10.0	332	32.2
4/7/11	-2.0	50.6	24.4	-2.0	368	23.8	-2.0	125	25.5
5/7/11	-1.0	373	24.7	-2.0	284.8	20.1	-2.0	358.2	23.0

Additional thermal and chemical treatments improved the $I-V$ characteristics of the structures (Fig. 5). The value of I_{sc} increased after the chemical etching of the prepared

structures in the mixture of 5 % KCN and 0.5 % KOH. A second annealing in the atmosphere of H₂ for 2 hours led to an additional increase of V_{oc} and FF (Figure 23).

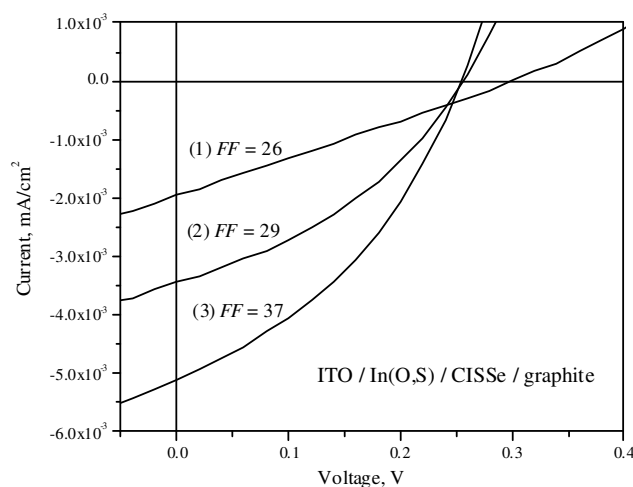


Figure 23. Dark and photo J - V characteristics for the photovoltaic device: (1) annealed at 450°C 30 min on H₂S, (2) annealed on H₂S and chemically etched in 5% KCN and 0.5% KOH, (3) annealed on H₂S, chemically etched, and additionally annealed at 450°C for 2 hours in the H₂ atmosphere.

4.4.2. ITO/In(O,S)/CuIn(S,Se)₂/POLYMERS PHOTOVOLTAIC STRUCTURE

The new approach to prepare the solar cell with organic polymer window was presented in Article IV. The principal scheme of the developed solar cell structure is shown in Figure 24. The advantage of this structure is the transparent contact on the top of the cell (transparent conductive polymer).

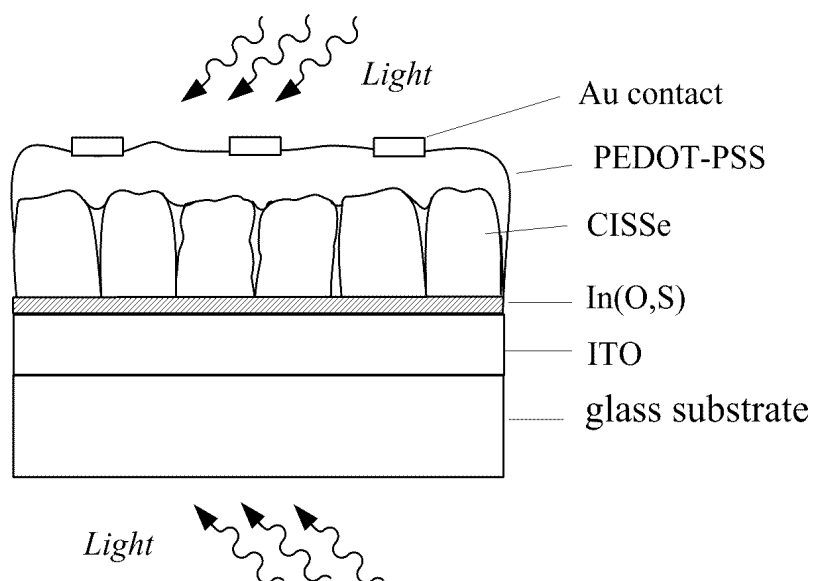


Figure 24. Schematic structure of ITO/In(O,S)/CuIn(S,Se)₂/PEDOT-PSS/Au-grid solar cell

The performance of the ITO/In(O,S)/CuIn(S_xSe_{1-x})₂ solar cells with and without window polymer layers was tested under illumination through the glass/ITO substrate and through the Au-grid front contact (look for data in Table 8). It was observed that the conductive polymer window layer improves the photovoltaic characteristics of the structures if an Au-grid top electrode is used. For the structure ITO/In(O,S)/ CuIn(S,Se)₂ /PEDOT-PSS/Au-grid, the values of parameters as high as $I_{sc} = 12.7 \text{ mA/cm}^2$ and $V_{oc} = 234 \text{ mV}$ were measured.

Table 8. Photovoltaic characteristics of different samples measured under the front (f) and back (b) illumination

Sample	ITO/In(O,S)/CuIn(S,Se) ₂ /Au		ITO/In(O,S)/ CuIn(S,Se) ₂ /PEDOT-PSS/Au	
	I_{sc} (mA/cm ²)	V_{oc} (mV)	I_{sc} (mA/cm ²)	V_{oc} (mV)
1	2.1 (f)	24.5 (f)	9.9 (f)	194 (f)
1	3.0 (b)	43.8 (b)	8.1 (b)	216.5 (b)
2	3.5 (b)	136.4 (b)	13.1 (b)	179.6 (b)
3	0.5 (b)	3 (b)	12.7 (f)	234.2 (f)
3			5.5 (b)	258.8 (b)

A considerable increase of I_{sc} and V_{oc} values was observed for the structures with an interfacial PEDOT layer. According to our assumption, this phenomenon is connected with the insulation of shunting paths through the deep micropores and cracks in the CuIn(S,Se)₂ layer by PEDOT (Figure 23).

4.4.3. ITO/CuInSe₂/POLYMERS PHOTOVOLTAIC STRUCTURES

Schematic drawing of ITO/CuInSe₂/Polymer/Ag photovoltaic structure is given in Figure 8. The structure is based on *n*-type of CuInSe₂ thin films and *p*-type conductive polymer (Articles VI,VII). The *n*-type CuInSe₂ films were deposited with an excess of In and annealed in vacuum. CuInSe₂ thin films with a thickness of about 1 μm were electrodeposited onto transparent ITO/glass substrates using the potentiostatic mode at -900 mV vs. SCE. Aqueous solutions containing CuSO₄ / In₂(SO₄)₃ / SeO₂ in concentrations of 2/8/11, 3/7/11 and 4/6/11 mM, respectively, were used as a source for the CuInSe₂ films deposition. The photoelectrochemical characterization in 0.1 M solution of H₂SO₄ of CuInSe₂ films confirmed the *n* -type conductivity of the films (Article V). The high-quality adhesive PPy films with a thickness of about 1 μm were electrodeposited galvanostatically onto *n*-CuInSe₂ films. The *p*-PANI layer was cast onto the glass/ITO/*n*-CuInSe₂ substrate from PANI solution in chloroform.

After the deposition of the PPy film onto the polycrystalline CuInSe₂ layer, an essential smoothening of the granular surface by the amorphous polymer and deep adhesive penetration of PPy into CuInSe₂ were observed (Figure 25).

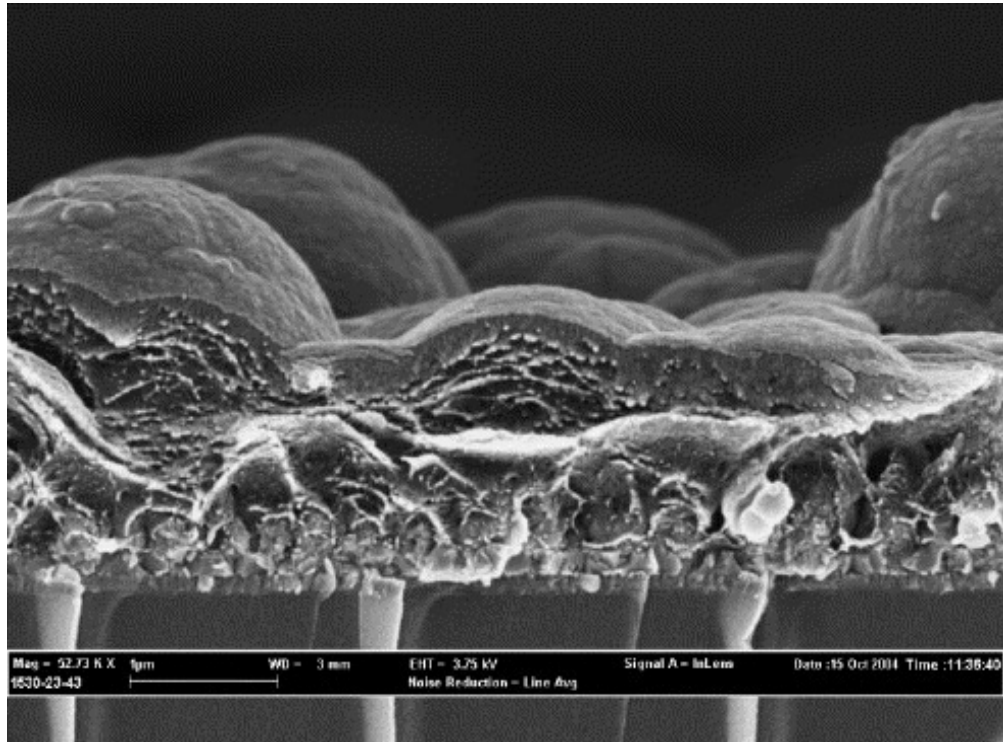


Figure 25. Cross-sectional SEM micrograph of glass/ITO/CuInSe₂/PPy structure

The complex impedance studies confirmed that a *n-p* barrier is formed between the *n*-CuInSe₂ and *p*-PPy layers (Article V). Figure 26 shows the photovoltaic properties of the obtained structures under white light illumination. The linearity of *I-V* characteristics of glass/ITO/ CuInSe₂/Polymer/Ag structures refer to a possibility that the photovoltaic behaviour could be fully controlled by the shunt resistance in the structure. The presence of these shunts influences the photovoltage markedly and restricts the values of V_{oc} and FF . The incident light produced a short-circuit photocurrent density I_{sc} and an open-circuit photovoltage V_{oc} with the values provided in Table 9. The best ITO/CuInSe₂/Polymer/metal structure showed $V_{oc} = 92$ mV and $I_{sc} = 1.70$ mA/cm² under white light illumination with 50 mW/cm²

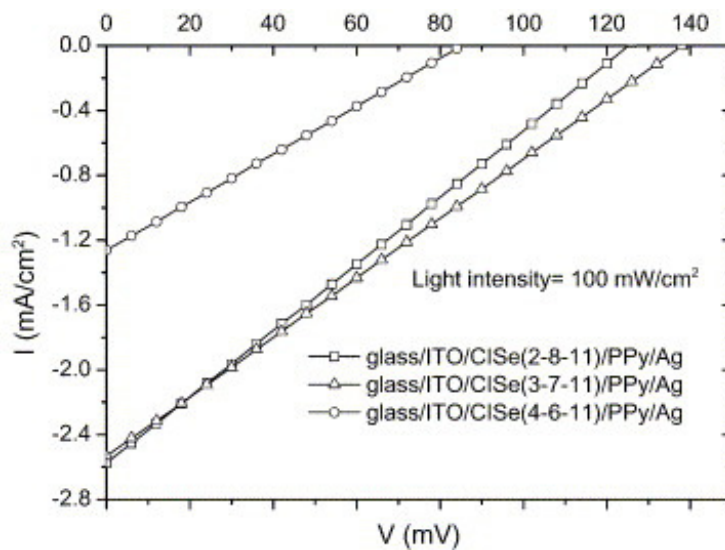


Figure 26. *I-V* characteristic of the glass/ITO/CuInSe₂/PPy/Ag photovoltaic structures under tungsten-halogen irradiance of 100 mW/cm²

Table 9. Parameters of the prepared ITO/CIS/PPy (PANI)/Ag photovoltaic structures

Structure	Cu/In/Se content in CuInSe ₂ (at. %)	V _{oc} (mV)	I _{sc} (mA/cm ²)
ITO / CIS (2-8-11) / PPy / Ag	7.9 / 40.5 / 51.6	83	1.71
ITO / CIS (3-7-11) / PPy / Ag	10.9 / 37.3 / 51.8	92	1.70
ITO / CIS (4-6-11) / PPy / Ag	13.1 / 36.0 / 50.9	57	0.84
ITO / CIS (1-3.3-3.3) / PANI / Ag	-	31	0.56

CONCLUSIONS

The following conclusion can be drawn from the results obtained:

1. A mechanism of CuInSe₂ formation through a number of consecutive reactions was composed. A possible path of reactions of compound formation is proposed. The formation of the Cu + Se phases precedes the assimilation of In and formation of CuInSe₂ compounds.
2. A theoretical model of the kinetics of the electrochemical deposition process was developed and the distribution diagram of components in the films deposited under diffusion limited current condition was calculated. Both theoretical calculations and experimental results are in good coincidence and confirm that the composition of thin films in electrochemical deposition is controlled by the composition of the electrolyte and the deposition potential.
3. The morphology of the electrodeposited films is determined by the over-potential cathodic voltage and by the rate of mass transport of solute species. The morphology and optical and electrical properties of annealed films could be tailored by the conditions of annealing (temperature, time and atmosphere of annealing).
4. The developed methods electrochemical etching in acidic and alkaline mediums are effective for removing of Cu₂Se phases from the film surface. Electrochemical etching in acidic and alkaline mediums allows additional removal of Cu₂Se phases from intergrain areas of films.
5. Two types of solar cells were prepared by help of electrochemical deposition of precursor CuInSe₂ thin films: photovoltaic structure on the base of *n*-In(O,S)/*p*-CuIn(S,Se)₂ junction and combined inorganic/organic - *n*-CuInSe₂/*p*-conductive polymer photovoltaic structure cells that are based on *n*-In(O,S)/*p*-CuIn(S,Se)₂ have the open circuit voltage (V_{oc}) up to 373 mV, whereas the short circuit current density (I_{sc}) is about 1mA/cm². The best structure based on the *n*-type of CuInSe₂ thin films and *p*-type polymer (polypyrrole) shows V_{oc} = 92 mV and I_{sc} = 1.70 mA/cm² under white light illumination with 50 mW/cm²

ACKNOWLEDGEMENTS

This thesis is based on the experimental work conducted at the Department of Materials Science, Tallinn University of Technology.

I would like to express my gratitude to all my colleagues for their contribution to this work. My special thanks are due to the following associates:

to my supervisor Prof. Enn Mellikov for his support, encouragement and advice during this work;

to Dr. Sergei Bereznev for help in preparation and investigation of organic photovoltaic structures;

to MSc. Olga Volobujeva for excellent SEM images and EDX analysis.

Support from the Estonian Ministry of Education and Research, Estonian Science Foundation (grants ETF 6162, 6179) and INTAS Project (nr. 03-51-4561) is greatly appreciated.

REFERENCES

-
- [1] D. Lincot, J.-F. Guillemoles, S. Taunier, D. Guimard, J. Sicx-Kurdi, A. Chaumont, O. Roussel, O. Ramdani, C. Hubert, J.P. Fauvarque et al., *Solar Energy*, 77 (2004) 725-737.
- [2] G. M. Barrow, *Physical Chemistry*, McGraw-Hill, (1961).
- [3] C. Hammann, A. Hamnett, W. Vielstich, *Electrochemistry*, Weinheim; New-York; Chichesster; Brisbane; Singapore; Toronto:Wiley-VCH , (1998).
- [4] F.A. Kröger, *J. Electrochem. Soc.*, 125 (1978) 2028.
- [5] G. F. Fulop, *Electrodeposition of Semiconductors*, *Ann. Rev. Mater. Sci.* 1985.15 : 197-210 Copyright © 1985 .
- [6] R.N. Bhattacharya, W. Batchelor, H. Wiesner et al., *J. Electrochem. Soc*, 145 (1998) 3435-3440.
- [7] M. Ganchev, J. Kois, M. Kaelin, S. Bereznev, E. Tzvetkova, O. Volobujeva, N. Stratieva, A. Tiwari, *Thin Solid Films*, 512 (2006) 325-327.
- [8] J. Penndorf, M. Winkler, O. Tober, D. Röser and K. Jacobs, *Sol. Energy Mat. and Sol. Cells*, 53 (1998) 285–298.
- [9] V.J. Kapur, B.M. Basol, E.S. Tseng, H.L., Hwang, et al. (Eds.), *Proceedings Seventh International Conf. Ternary and Multinary Compounds*, (1987) 219–224.
- [10] A. Gupta, S. Shirakata, S. Isomura, *Sol. Energy Mat. and Sol. Cells*, 32 (1994) 137-149.
- [11] S.R. Kumar, R.B. Gore, R.K. Pandey, *Sol. Energy Mat. and Sol. Cells*, 26 (1992) 149-158.
- [12] E. Calixto, P. J. Sebastian and A. Fernandez, *J. Crystal Growth.*, 169 (1996) 287-292.
- [13] R.P. Wijesundera and W. Siripala, *Sol. Energy Mat. and Sol. Cells*, 81 (2004) 147-154.
- [14] R. Friedfeld, R.P. Raffaele and J.G. Mantovani, *Sol. Energy Mat. and Sol. Cells*, 58 (1999) 375-385.
- [15] S. Massaccesi, S. Sanchez and J. Vedel, *J. Electroanal. Chem.* 412 (1996) 95–101.
- [16] J. Vedel, *Ternary and Multinary Compounds. Proceedings of the 11th International Conference on Ternary and Multinary Compounds. ICTMC-11 (1998)* 261-268.
- [17] S. Massaccesi, S. Sanchez and J. Vedel, *J. Electrochem. Soc.*, 140 (1993) 2540-2546.
- [18] D. Lippkow and H.-H. Strheblow, *Electrochimica Acta*, 43 (1998) 2131 -2140
- [19] C.D. Lokhade , *B. Electrochem*, 3 (1987) 219-223.
- [20] A.M. Hermann, M. Mansour, V. Badri, B. Pinkhasov, C. Gonzales, F. Fickett, M.E. Calixto, P.J. Sebastian, C. H. Marshall and T. J. Gillespie, *Thin Solid Films*, 361 (2000) 74-78.
- [21] A.M. Fernandez, M.E. Calixto, P.J. Sebastian, S.A. Gamboa, A.M. Hermann and R.N. Noufi, *Solar Energy materials*, 52 (1998) 423-431.
- [22] A.M. Hermann, R. Westfall and R. Wind, *Sol. Energy Mat. and Sol. Cells*, 52 (1998) 355-360.
- [23] R.N. Bhattacharya, *J. Electrochem. Soc.* 130 (1983) 2040-2042.
- [24] N.B. Chaure, J. Young, A.P. Samantilleke and I.M. Dharmadasa, *Sol. Energy Mat. and Sol. Cells*, 81 (2004) 125-133.
- [25] A.A.I. Al-Bassam, *Physica B: Condensed Matter*, 266 (1999) 192-197.

- [26] A.M. Fernandez, P.J. Sebastian, M.E. Calixto, S.A. Gamboa and O. Solorza, *Thin Solid Films*, 298 (1997) 92-97.
- [27] M.E. Calixto, P.J. Sebastian, R.N. Bhattacharya and R. Noufi, *Sol. Energy Mat. and Sol. Cells*, 59 (1999) 75-84.
- [28] R. Friedfeld, R.P. Raffaele and J.G. Mantovani, *Sol. Energy Mat. and Sol. Cells*, 58 (1999) 375-385.
- [29] R.N. Bhattacharya and A.M. Fernandez, *Sol. Energy Mat. and Sol. Cells*, 76 (2003) 331-337.
- [30] A.M. Martinez, L.G. Arriaga, A.M. Fernández and U. Cano, *Materials Chemistry and Physics*, 88 (2004) 417-420.
- [31] T. Yukawa, K. Kuwabara and K. Koumoto, *Thin Solid Films*, 286 (1996) 151-153.
- [32] S. Nakamura and A. Yamamoto, *Sol. Energy Mat. and Sol. Cells*, 75 (2003) 81-86.
- [33] T. Edamura and J. Muto, *J. Mater. Sci. Lett.* 14 (1995) 1400-1402.
- [34] T. Ishizaki, N. Saito and A. Fuwa, *Surf. Coat. Technol.*, 182 (2004) 156-160.
- [35] R. Diaz, J.M. Merino, F. Rueda, P. Ocon and P. Herrasti, *J. Mater. Chem.*, 10 (2000) 1623-1627.
- [36] L. Thouin, S. Massaccesi, S. Sanchez and J. Vedel, *J. Electroanal. Chem.*, 374 (1994) 81-88.
- [37] K.K. Mishra and K. Rajesvar, *J. Electroanal. Chem.*, 271 (1989) 279-294.
- [38] J.-F. Guillemoles, R. Diaz, P. Cowache, L. Thouin, D. Lincot And J. Vedel 13th european photovoltaic solar energy converence and exibition Nice, France, 1995.
- [39] R.P. Singh, S.L. Singh and S. Chandra, *J. Phys. D: Appl. Phys.* 19 (1986) 1299-1309.
- [40] L. Thouin, S. Rouquette-Sanchez and J. Vedel, 10th european photovoltaic solar energy conference (1991) 893-896.
- [41] S.N. Sahu, R.D.L. Kristennesen and D. Haneman, *Solar Energy materials*, 18 (1989) 385-397.
- [42] S. M. Babu, R. Dhanasekara and P. Ramasamy, *Thin Solid Films*, 198 (1991) 269-278.
- [43] J. Vedel, L. Thouin and D. Lincot, *J. Electrochem. Soc.* 143 (1996) 2173-2180.
- [44] C. Guillen and J. Herrero, *J. Electrochem. Soc.* 141 (1994) 225-230.
- [45] L. Thouin and J. Vedel, *J. Electrochem. Soc.* 142 (1995) 2996-3000.
- [46] Y. Ueno, H. Kawai, T. Sugiura and H. Minoura, *Thin Solid Films*, 157 (1988) 159-168.
- [47] A. N. Molin, A. I. Dikumar, G. A. Kiosse, P. A. Petrenko, A. I. Sokolovsky and Yu. G. Saltanovsky, *Thin Solid Films*, 237 (1994) 66-71.
- [48] A.N. Molin, and A.I. Dikumar, *Thin Solid Films*, 237 (1994) 72-77.
- [49] J.-F. Guillemoles, P.C. Cowache, A. Lussion, K. Fezzaa, F. Boisivion, J. Vedel, D. Lincot, *J. Appl. Phys.*, 79 (1996) 7293-7301.
- [50] L. Thouin, J.-F. Guillemoles, S. Massaccesi, R. Ortega Borges, S. Sanchez, P. Cowache, D. Lincot and J. Vedel., *Solid State Phenomena*, 37/38 (1994) 527-532.
- [51] N. Khare, G. Razzini, L. Peraldo Bicelli, *Solar Cells*, 31 (1991) 283-295.
- [52] S.N. Qiu, L. Li, C.X. Qiu, I. Shih, and C.H. Champness, *Sol. Energy Mat. and Sol. Cells*, 37 (1995) 389-393.
- [53] P. Garg, A. Garg, A.C. Rastogi and J.C. Garg, *J. Phys. D: Appl. Phys.*, 24 (1991) 2026-2031.
- [54] T. Pottier, and G. Maurin, *J. Appl. Electrochem.*, 19 (1989) 361-367.
- [55] R.N. Bhattacharya, J.F. Hiltner, W. Batchelor, M.A. Contreras, R.N. Noufi and J.R. Sites, *Thin Solid Films*, 361 (2000) 396-399.

- [56] D. Haneman, S. Sahu, R.D.L. Krisensen, 7th International Conference on Thin Films, New Delhi, India December 7-11, 1987.
- [57] R. Ugarte, R. Schrebler, R. Cordova, E.A. Dalchiele and H. Gomez, *Thin Solid Films*, 340 (2000) 117–124.
- [58] M.C.F. Oliveira, M. Azevedo, A. Cunha, *Thin Solid Films*, 405 (2002) 129-134.
- [59] N. Stratieva, E. Tzvetkova, M. Ganchev, K. Kochev and I. Tomov, *Sol. Energy Mat. and Sol. Cells*, 45 (1997) 87–96.
- [60] M. Kemell, M. Ritala, H. Saloniemi, M. Leskela, T. Sajavaara and E. Rauhala, *J. Electrochem. Soc.* 147 (2000) 1080–1087.
- [61] S. Siebentritt, *Thin Solid Films*, 403 (2002) 1-8.
- [62] T. Gödecke, T. Haalboom, F. Ernst *Zeitschrift für Metallkunde*, 91 (2000) 622–662.
- [63] H. Neumann and R.D. Tomlinson, *Solar Cells*, 28 (1990) 301–313.
- [64] S. Isomura, A. Nagamatsu, K. Shinohara and T. Aono, *Solar Cells*, 16 (1986) 143-153.
- [65] J-F. Guillemoles A. Lusso, P. Cowache, S. Massaccesi, J. Vedel , D. Lincot, *Adv. Mater.*, 6 (1994) 376-379.
- [66] H. Matsushita, A. Katsui and T. Takizawa, *J. Crystal Growth*, 237 (2002) 1986-1992.
- [67] P. J. Sebastian, M. E. Calixto, R. N. Bhattacharya and R.Noufi, *Sol. Energy Mat. and Sol. Cells*, 59 (1999) 125-135.
- [68] M. E. Calixto, R. N. Bhattacharya, P. J. Sebastian, A. M. Fernandez, S. A. Gamboa and R. N. Noufi *Sol. Energy Mat. and Sol. Cells*, 55 (1998) 23-29.
- [69] A. Gupta and S. Isomura, *Sol. Energy Mat. and Sol. Cells*, 53 (1998) 385-401.
- [70] A. Kampmann, V. Sittinger, J. Rechid and R. Reineke-Koch, *Solid Films*, 361 (2000) 309–313.
- [71] R.N. Bhattacharya, W. Batchelor, J.F. Hiltner and J.R. Sites, *J. Appl. Phys. Lett.* 75 (1999) 1431–1433.
- [72] M. E. Calixto, R. N. Bhattacharya, P. J. Sebastian, A. M. Fernandez, S. A. Gamboa and R. N. Noufi, *Sol. Energy Mat. and Sol. Cells*, 55 (1998) 23-29.
- [73] K.T.L. De Silva, W.A.A. Priyantha, J.K.D.S. Jayanetti, B.D. Chithrani, W. Siripala, K. Blake and I.M. Dharmadasa, *Thin Solid Films*, 382 (2001) 158-163.
- [74] E. Tzvetkova, N. Stratieva, M. Ganchev, I. Tomov, K. Ivanova and K. Kochev, *Thin Solid Films*, 311 (1997) 101–106.
- [75] C. Guillen and J. Herrero, *J. Electrochem. Soc.* 143 (1996) 493–498.
- [76] D. Lincot, J.F. Guillemoles, P. Cowache, S. Massaccesi, L. Thouin, K. Fezzaa, F. Boisivon, J. Vedel, *Conference Record of the IEEE Photovoltaic Specialists Conference 1*, (1994) 136–139.
- [77] J.F. Guillemoles, P. Cowache, S. Massaccesi, L. Thouin, S. Sanchez, D. Lincot and J. Vedel, *Adv. Mater.* 6 (1994) 379–381
- [78] N. Stratieva, E. Tzvetkova, M. Ganchev, K. Kochev and I. Tomov, *Sol. Energy Mat. and Sol. Cells*, 45 (1997) 87–96.
- [79] C. Guillen and J. Herrero, *Sol. Energy Mat. and Sol. Cells*, 43 (1996) 47–57.
- [80] L. Zhang, F. D. Jiang and J. Y. Feng, *Sol. Energy Mat. and Sol. Cells*, 80 (2003) 483-490.
- [81] F.O. Adurodija, M.J. Carter and R. Hill, *Sol. Energy Mat. and Sol. Cells*, 40 (1996) 359-369.
- [82] N.A. Zeenath, P.K.V. Pillai, K. Bindu, M. Lakshmy, K.P. Vijayakumar, *J. Mat. Sci.*, 35 (2000) 2619 – 2624.
- [83] A. Ashour, A. A. S. Akl, A. A. Ramadan and K. Abd EL-Hady, *Thin Solid Films*, 467 (2004) 300-307.

- [84] J. Sterner, Th.W. Matthes, J. Kessler, J. Lu, J. Keranen, E. Olsson, L. Stolt, Proceedings of the 16th European Photovoltaic Solar Energy Conference and Exhibition (2000) 771-774.
- [85] J. Keränen, J. Lu, J. Barnard, J. Sterner, J. Kessler, L. Stolt, Th. W. Matthes and E. Olsson, *Thin Solid Films*, 387 (2001) 80-82.
- [86] B. Canava, J. F. Guillemoles, J. Vigneron, D. Lincot and A. Etcheberry, *J. Phys. and Chem. of Solids*, 64 (2003) 1791-1796.
- [87] K. Müller, R. Scheer, Y. Burkov and D. Schmeißer, *Thin Solid Films*, 451 (2004) 120-123.
- [88] S. Percharmant, J.-F. Guillemoles, J. Vedel, D. Lincot, 11th Int. Conf. on Ternary and Multinary Compounds ICTMC-11 Salford, 1997, 719.
- [89] T. Delsol, M. C. Simmonds and I. M. Dharmadasa, *Sol. Energy Mat. and Sol. Cells*, 77 (2003) 331-339.
- [90] T. Wilhelm, B. Berenguier, M. Aggour, K. Skorupska, M. Kanis, M. Winkelkemper, J. Klaer, C. Kelch and H.-J. Lewerenz, *Thin Solid Films*, 480 (2005) 24-28.
- [91] B. Berenguier and H.J. Lewerenz, *Electrochemistry Communications*, 8 (2006) 165-169.
- [92] U. Störkel, M. Aggour, C.P. Murrell and H.J. Lewerenz, *Thin Solid Films*, 387 (2001) 182-184.
- [93] H. Kushiya, M. Tachiyuki, Y. Nagoya, A. Fujimaki, B. Sang, D. Okimura, M. Satoh, O. Yamase, in: *Proceedings of the Technical Digest on International PVSEC-11, Sapporo 1999*, 637.
- [94] A.J. Frank, S. Glenis, A.J. Nelson, *J. of Phys. Chem.*, 93 (1989) 3818.
- [95] P. Chartier, H. Nguyen Cong, C. Sene, *Solar Energy Materials and Solar Cells*, 52 (1998) 413.
- [96] P.J. Sebastian, S.A. Gamboa, M.E. Calixto, H. Nguyen-Cong, P. Chartier, R. Perez, *Semiconductors Science and Technology*, 13 (1998) 1459.
- [97] D. Hariskos, S. Spiering and M. Powalla, *Thin Solid Films*, 480 (2005) 99-109.
- [98] Jr. C.F. Baes and R.E., Mesmer, *The Hydrolysis of Cations*, Wiley-Interscience, New York 1976. p. 489
- [99] L.T. Vlaev, M.M. Nikolova and G.G. Gospodinov, *J. Solid State Chemistry*, 177 (2004) 2663-2669.
- [100] V. P. Verma, *Thermochemica Acta*, 327 (1999) 63-102.
- [101] H.V. Rasika Dias, Indium and Thallium, *Comprehensive Coordination Chemistry II*, 2004, Chapter 3.5, 383-463
- [102] R.R. Nazmutdinov, T.T. Zinkicheva, G.A. Tsirlina and Z.V. Kuz'minova, *Electrochimica Acta*, 50 (2005) 4888-4896.
- [103] F. Séby, M. Potin-Gautier, E. Giffaut, G. Borge and O. F. X. Donard, *Chemical Geology*, 171 (2001) 173-194.
- [104] D. Schmid, M. Ruckh, F. Grunwald, and H. W. Schock, *J. Appl. Phys.*, 73 (1993) 2902-2909.
- [105] J. Kois, S. Bereznev, E. Mellikov and A. Opik, 3rd World Conference on Photovoltaic Energy Conference (WCPE-3, May 11-18, 2003 Osaka, Japan) proceedings.
- [106] T. Walter and H.W. Schock, *Thin Solid Films*, 224 (1993) 74-81.
- [107] R. Diaz, M. Leon, *J. Appl. Phys.*, 1996. 80 (7) 5610.
- [108] C. Guillén and J. Herrero, *Solar Energy Materials and Solar Cells*, 73 (2002) 141-149.

- [109] R.C. Valderrama, P.J. Sebastian, J. Pantoja Enriquez and S.A. Gamboa, Sol. Energy Mat. and Sol. Cells, 88 (2005) 145-155.

APPENDIX

- I. J. Kois, S. Bereznev, E. Mellikov and A. Öpik, Electrodeposition of CuInSe₂ thin films onto Mo-glass substrates, Thin Solid Films, Vol. 511-512, 26 July 2006, pp 420-424.
- II. J. Kois, S. Bereznev, O. Volobujeva, E. Mellikov, Electrochemical Etching of Copper Indium Diselenide Surface, The E-MRS 2006 Spring Meeting Nice (France), from May 29 to June 2, 2006, Thin Solid Films, accepted.
- III. Julia Kois, Sergei Bereznev, Enn Mellikov, and Andres Öpik, Photovoltaic structures formed by thermal annealing of electrodeposited CuInSe₂ in H₂S, Proceedings of the Estonian Academy of Sciences, Chemistry, Vol. 52 No. 2 June 2003, pp. 51–58.
- IV. J. Kois, S. Bereznev, J. Raudoja, E. Mellikov and A. Öpik, Glass/ITO/In(O,S)/CuIn(S,Se)₂ solar cell with conductive polymer window layer, Solar Energy Materials and Solar Cells, Vol. 87, Issues 1-4, May 2005, pp. 657-665.
- V. S. Bereznev, J. Kois, I. Golovtsov, A. Öpik and E. Mellikov, Electrodeposited (Cu–In–Se)/polypyrrole PV structures, Thin Solid Films, Vol. 511-512, 26 July 2006, pp. 425-429.
- VI. S. Bereznev, J. Kois, E. Mellikov, A. Öpik and D. Meissner, CuInSe₂/Polypyrrole Photovoltaic Structure Prepared by Electrodeposition, Proceedings of 17th European Photovoltaic Solar Energy Conference (Munich, Germany, October 22-26, 2001), 1 (2002), pp. 160-163.
- VII. S. Bereznev, J. Kois, E. Mellikov, A. Öpik, CuInSe₂/Polyaniline Photovoltaic Structure, Proceedings of Baltic Polymer Symposium 2001, Tallinn, Estonia, October 11-12, 2001, pp. 148-154.

CURRICULUM VITAE

Name: **Julia Kois**
Date of Birth: 24. 09. 1971
Address: Tallinn, Kolde 104-90;
Telephone: +372 55 606 309;
e-mail: julia@staff.ttu.ee

Education

Tallinn University of Technology, Department of Chemistry, *PhD student*,
"Electrochemical Deposition of CuInSe₂ Thin Films for Photovoltaic Applications",
(September 2002 - present)

Tallinn University of Technology, Department of Chemistry, *Master of Natural Sciences*,
"Electrochemical Deposition of CuInSe₂ Thin Films for Photovoltaic Applications", 2000

Tallinn University of Technology, Department of Chemistry, *Bachelor of Natural Sciences*, 1996

Employment

Tallinn University of Technology, Department of Materials Science

Researcher (since 1998)

Graduate engineer 1995-1998

Publication

1. M. Ganchev, J. Kois, M. Kaelin, S. Bereznev, E. Tzvetkova, O. Volobujeva, N. Stratieva and A. Tiwari, **Preparation of Cu(In,Ga)Se₂ layers by selenization of electrodeposited Cu-In-Ga precursors**, Thin Solid Films, Volumes 511-512, 26 July 2006, Pages 325-327
2. J. Kois, S. Bereznev, E. Mellikov and A. Öpik, **Electrodeposition of CuInSe₂ thin films onto Mo-glass substrates**, Thin Solid Films, Volumes 511-512, 26 July 2006, Pages 420-424
3. S. Bereznev, J. Kois, I. Golovtsov, A. Öpik and E. Mellikov, **Electrodeposited (Cu-In-Se)/polypyrrole PV structures**, Thin Solid Films, Volumes 511-512, 26 July 2006, Pages 425-429
4. A. Verbitsky, Ya. Vertsimakha, P. Lutsyk, S. Studzinsky, S. Bereznev, J. Kois, A. Öpik, and E. Mellikov, **Properties of CuInS₂ free surface and effect of conductive polymer layers on these properties**, Proceedings of the Estonian Academy of Sciences, Chemistry, 55 (2006) 111-119

5. J. Kois, S. Bereznev, O. Volobujeva, E. Mellikov, **Electrochemical Etching of Copper Indium Diselenide Surface**, The E-MRS 2006 Spring Meeting Nice (France), from May 29 to June 2, 2006, to be published
6. S. Bereznev, I. Konovalov, A. Öpik, J. Kois and E. Mellikov, **Hybrid copper-indium disulfide/polypyrrole photovoltaic structures prepared by electrodeposition**, Solar Energy Materials and Solar Cells, Volume 87, Issues 1-4, May 2005, Pages 197-206
7. J. Kois, S. Bereznev, J. Raudoja, E. Mellikov and A. Öpik **Glass/ITO/In(O,S)/CuIn(S,Se)₂ solar cell with conductive polymer window layer**, Solar Energy Materials and Solar Cells, Volume 87, Issues 1-4, May 2005, Pages 657-665
8. S. Bereznev, I. Konovalov, J. Kois, E. Mellikov, A. Öpik, **Polypyrrole electrodeposition on Inorganic Semiconductors CuInSe₂ and CuInS₂ for Photovoltaic Applications**, Macromol. Symp. 2004, 212, 287-292.
9. A. Verbitsky, Ya. Vertsimakha, P. Lutsyk, S. Studzinsky, S. Bereznev, J. Kois, **Properties of CuInS₂ Free Surface and Effect of Organic Layers**, Semiconductors, 40, Nr. 2 (2006), 197-201.
10. Julia Kois, Sergei Bereznev, Enn Mellikov, and Andres Öpik, **Photovoltaic structures formed by thermal annealing of electrodeposited CuInSe₂ in H₂S**, Proceedings of the Estonian Academy of Sciences, Chemistry, Vol. 52 No. 2 June 2003, p. 51-58.
11. J. Kois, S. Bereznev, M. Altosaar, E. Mellikov, A. Öpik, **Electrodeposition of CuInSe₂ thin films**, Proceedings of 3rd World Conference on Photovoltaic Energy Conference (WCPEC-3, May 11-18, 2003, Osaka, Japan) on CD-ROM, article 2P-A8-09, 4 pages.
12. S. Bereznev, J. Kois, E. Mellikov, A. Öpik and D. Meissner, **CuInSe₂/Polypyrrole Photovoltaic Structure Prepared by Electrodeposition**, Proceedings of Seventeenth European Photovoltaic Solar Energy Conference (München, Germany, October 22-26, 2001), 1 (2002), p. 160-163.
13. S. Bereznev, J. Kois, E. Mellikov, A. Öpik, D. Meissner, **CuInSe₂/polypyrrole (polyaniline) photovoltaic structures**, Proceedings of the 14th Workshop on Quantum Solar Energy Conversion - QUANTSOL 2002, Rauris, Austria, March 17-23, 2002, p. 59.
14. S. Bereznev, J. Kois, E. Mellikov, A. Öpik, **CuInSe₂/Polyaniline Photovoltaic Structure**, Proceedings of Baltic Polymer Symposium 2001, Tallinn, Estonia, October 11-12, 2001, p. 148-154.
15. J. Kois, S. Bereznev, E. Mellikov and A. Öpik, **Electrodeposition of CuInSe₂ Thin Films onto Mo-glass Substrates**, Thin Solid Films, 511-512, (2006), pp 420-424.
16. E. Mellikov, M. Altosaar, S. Bereznev, M. Kauk, J. Kois, J. Krustok, M. Krunks, and T. Varema, **Materials and technologies for photovoltaic applications from Estonia**, Proceedings of SPIE, Optical Materials and Applications, 5946 (2005) pp. 59460X-1 – 59460X-9.
17. J. Kois, S. Bereznev, E. Mellikov and A. Öpik, **Electrodeposition of thin film CuInSe₂**, 3rd World Conference on Photovoltaic Energy Conference (WCPEC-3, May 11-18, 2003 Osaka, Japan) proceedings.

ELULOOKIRJELDUS

Ees- ja perekonnanimi: **Julia Kois**
Sünniaeg ja koht: 24. 09. 1971, Venemaa
Aadress: Tallinn, Kolde 104-90;
Telefon: +372 55 606 309;
e-mail: julia@staff.ttu.ee

Hariduskäik

Tallinna Tehnikaülikool, *Doktorantuur*, keemia- ja materjalitehnoloogia, doktoritöö tema "CuInSe₂ õhukesed kiled elektrokeemilise sadestamise meetodil" (alates september 2002)

Tallinna Tehnikaülikool, *Loodusteaduste magister*, keemia- ja materjalitehnoloogia, 2000

Tallinna Tehnikaülikool, *Loodusteaduste bakalaureus*, pooljuhtmaterjalide tehnoloogia, 1996

Täiendkoolitused

Helsinki Teadusülikool 1998,
Jülichi teaduskeskus, Saksamaa, 1999,
Bulgaaria TA Päikeseenergeetika 2004.

Töökogemus

Tallinna Tehnikaülikool, materjaliteaduse instituut

Teadur alates 1998
Insener 1995-1998

Publikatsioonid

1. M. Ganchev, J. Kois, M. Kaelin, S. Bereznev, E. Tzvetkova, O. Volobujeva, N. Stratieva and A. Tiwari, **Preparation of Cu(In,Ga)Se₂ layers by selenization of electrodeposited Cu–In–Ga precursors**, *Thin Solid Films, Volumes 511-512, 26 July 2006, Pages 325-327*
2. J. Kois, S. Bereznev, E. Mellikov and A. Öpik, **Electrodeposition of CuInSe₂ thin films onto Mo-glass substrates**, *Thin Solid Films, Volumes 511-512, 26 July 2006, Pages 420-424*
3. S. Bereznev, J. Kois, I. Golovtsov, A. Öpik and E. Mellikov, **Electrodeposited (Cu–In–Se)/polypyrrole PV structures**, *Thin Solid Films, Volumes 511-512, 26 July 2006, Pages 425-429*

4. A. Verbitsky, Ya. Vertsimakha, P. Lutsyk, S. Studzinsky, S. Bereznev, J. Kois, A. Öpik, and E. Mellikov, **Properties of CuInS₂ free surface and effect of conductive polymer layers on these properties**, Proceedings of the Estonian Academy of Sciences, Chemistry, 55 (2006) 111-119
5. J. Kois, S. Bereznev, O. Volobujeva, E. Mellikov, **Electrochemical Etching of Copper Indium Diselenide Surface**, The E-MRS 2006 Spring Meeting Nice (France), from May 29 to June 2, 2006, aktsepteeritud publikatsioon
6. S. Bereznev, I. Konovalov, A. Öpik, J. Kois and E. Mellikov, **Hybrid copper–indium disulfide/polypyrrole photovoltaic structures prepared by electrodeposition**, *Solar Energy Materials and Solar Cells, Volume 87, Issues 1-4, May 2005, Pages 197-206*
7. J. Kois, S. Bereznev, J. Raudoja, E. Mellikov and A. Öpik **Glass/ITO/In(O,S)/CuIn(S,Se)₂ solar cell with conductive polymer window layer**, *Solar Energy Materials and Solar Cells, Volume 87, Issues 1-4, May 2005, Pages 657-665*
8. S. Bereznev, I. Konovalov, J. Kois, E. Mellikov, A. Öpik, **Polypyrrole electrodeposition on Inorganic Semiconductors CuInSe₂ and CuInS₂ for Photovoltaic Applications**, Macromol. Symp. 2004, 212, 287-292.
9. A. Verbitsky, Ya. Vertsimakha, P. Lutsyk, S. Studzinsky, S. Bereznev, J. Kois, **Properties of CuInS₂ Free Surface and Effect of Organic Layers**, Semiconductors, 40, Nr. 2 (2006), 197-201.
10. Julia Kois, Sergei Bereznev, Enn Mellikov, and Andres Öpik, **Photovoltaic structures formed by thermal annealing of electrodeposited CuInSe₂ in H₂S**, *Proceedings of the Estonian Academy of Sciences, Chemistry, Vol. 52 No. 2 June 2003, p. 51–58*.
11. J. Kois, S. Bereznev, M. Altosaar, E. Mellikov, A. Öpik, **Electrodeposition of CuInSe₂ thin films**, Proceedings of 3rd World Conference on Photovoltaic Energy Conference (WCPEC-3, May 11-18, 2003, Osaka, Japan) on CD-ROM, article 2P-A8-09, 4 pages.
12. S. Bereznev, J. Kois, E. Mellikov, A. Öpik and D. Meissner, **CuInSe₂/Polypyrrole Photovoltaic Structure Prepared by Electrodeposition**, Proceedings of Seventeenth European Photovoltaic Solar Energy Conference (München, Germany, October 22-26, 2001), 1 (2002), p. 160-163.
13. S. Bereznev, J. Kois, E. Mellikov, A. Öpik, D. Meissner, **CuInSe₂/polypyrrole (polyaniline) photovoltaic structures**, Proceedings of the 14th Workshop on Quantum Solar Energy Conversion - QUANTSOL 2002, Rauris, Austria, March 17-23, 2002, p. 59.
14. S. Bereznev, J. Kois, E. Mellikov, A. Öpik, **CuInSe₂/Polyaniline Photovoltaic Structure**, Proceedings of Baltic Polymer Symposium 2001, Tallinn, Estonia, October 11-12, 2001, p. 148-154.
15. J. Kois, S. Bereznev, E. Mellikov and A. Öpik, **Electrodeposition of CuInSe₂ Thin Films onto Mo-glass Substrates**, Thin Solid Films, 511-512, (2006), pp 420-424.
16. E. Mellikov, M. Altosaar, S. Bereznev, M. Kauk, J. Kois, J. Krustok, M. Krunks, and T. Varema, **Materials and technologies for photovoltaic applications from Estonia**, Proceedings of SPIE, Optical Materials and Applications, 5946 (2005) pp. 59460X-1 – 59460X-9.

17. J. Kois, S. Bereznev, E. Mellikov and A. Öpik, **Electrodeposition of thin film CuInSe₂**, 3rd World Conference on Photovoltaic Energy Conference (WCPES-3, May 11-18, 2003 Osaka, Japan) proceedings.